CD70/CD27 signaling promotes blast stemness and is a viable therapeutic target in acute myeloid leukemia

Carsten Riether,[1,3]* Christian M. Schürch,[1,2]* Elias D. Bührer,[1] Magdalena Hinterbrandner,[1] Anne-Laure Huguenin,[1] Sabine Hoepner,[1] Inti Zlobec,[2] Thomas Pabst,[3] Ramin Radpour,[1] and Adrian F. Ochsenbein[1,3]

[1]Tumor Immunology, Department of Clinical Research and [2]Institute of Pathology, University of Bern, 3008 Bern, Switzerland
[3]Department of Medical Oncology, Inselspital, University Hospital and University of Bern, 3010 Bern, Switzerland

Aberrant proliferation, symmetric self-renewal, increased survival, and defective differentiation of malignant blasts are key oncogenic drivers in acute myeloid leukemia (AML). Stem cell gene signatures predict poor prognosis in AML patients; however, with few exceptions, these deregulated molecular pathways cannot be targeted therapeutically. In this study, we demonstrate that the TNF superfamily ligand–receptor pair CD70/CD27 is expressed on AML blasts and AML stem/progenitor cells. CD70/CD27 signaling in AML cells activates stem cell gene expression programs, including the Wnt pathway, and promotes symmetric cell divisions and proliferation. Soluble CD27, reflecting the extent of CD70/CD27 interactions in vivo, was significantly elevated in the sera of newly diagnosed AML patients and is a strong independent negative prognostic biomarker for overall survival. Blocking the CD70/CD27 interaction by mAb induced asymmetric cell divisions and differentiation in AML blasts and AML stem/progenitor cells, inhibited cell growth and colony formation, and significantly prolonged survival in murine AML xenografts. Importantly, hematopoietic stem/progenitor cells from healthy BM donors express neither CD70 nor CD27 and were unaffected by blocking mAb treatment. Therefore, targeting CD70/CD27 signaling represents a promising therapeutic strategy for AML.

INTRODUCTION

Acute myeloid leukemia (AML) is a group of genetically diverse and highly aggressive hematological malignancies characterized by the accumulation of immature blasts. AML represents the most common form of acute leukemia in adults and accounts for most leukemia-related deaths (Siegel et al., 2013; Döhner et al., 2015).

In recent years, genetic and molecular aberrations underlying AML pathogenesis have been identified. A first genetic alteration occurs in a hematopoietic stem/progenitor cell (HSPC), initiating clonal expansion. Subsequently, within this expanding clone, additional cooperating mutations are acquired, resulting in aberrant cell growth and a differentiation block (Jan et al., 2012; Corces-Zimmerman et al., 2014; Shlush et al., 2014; Vasanthakumar and Godley, 2014). The improved understanding of disease mechanisms has allowed defining biologically homogenous risk groups with regard to treatment response, disease relapse, and overall survival (Patel

et al., 2012; Zeisig et al., 2012). The current standard of care for the majority of AML patients is still a combination of cytarabine with an anthracycline. However, the characterization of molecular abnormalities in AML has led to the development of novel targeted agents, including FLT3, IDH1/2, and KIT inhibitors (Döhner et al., 2015).

AML is hierarchically organized and maintained by self-renewing leukemia stem cells (LSCs) that sustain a pool of disease-inducing cells (Reya et al., 2001; Huntly and Gilliland, 2005; Horton and Huntly, 2012). LSCs may self-renew symmetrically or divide asymmetrically into an LSC and a more differentiated progenitor. Changes in this balance toward symmetric self-renewal will lead to an accumulation of undifferentiated malignant cells with stem cell characteristics (Kreso and Dick, 2014; Bajaj et al., 2015). For example, this was shown for the progression of chronic myelogenous leukemia (CML) from chronic to blast phase where the fraction of symmetrically dividing cells increased (Jamieson et al., 2004; Wu et al., 2007; Bajaj et al., 2015). Concordantly, high LSC numbers as well as stem cell gene signatures in blasts are negative predictors for survival (van Rhenen et al., 2005; Pearce et al., 2006; Gentles et al., 2010; Eppert et al., 2011). Therefore, target-
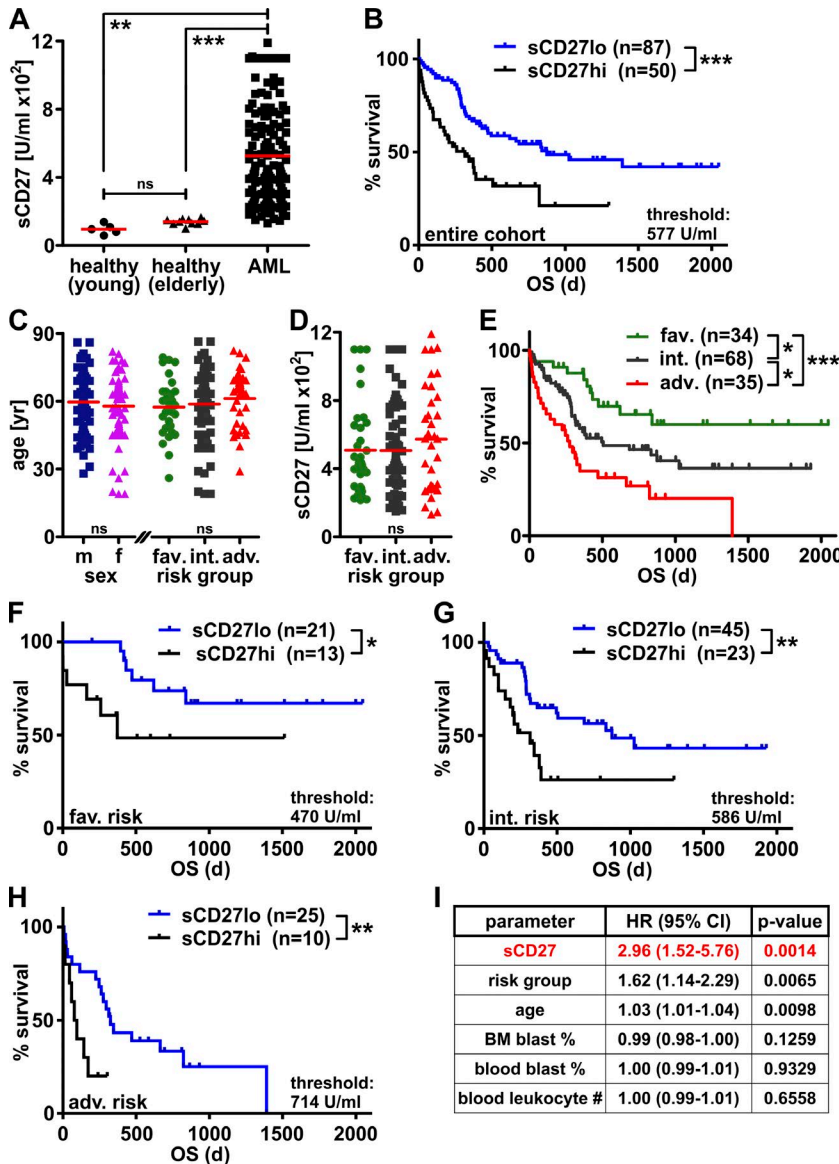
The Journal of Experimental Medicine

Figure 1. **sCD27 is an independent negative prognostic biomarker in AML.** (A) sCD27 levels in serum samples from newly diagnosed AML patients (*n* = 137), young (*n* = 5, mean of technical duplicates) and elderly (*n* = 10) healthy control subjects. (B) Kaplan-Meier survival curves of the entire AML patient cohort (*n* = 137) divided into two groups at the sCD27 threshold of 577 U/ml. (C) Patient age at diagnosis, differentiated according to sex (left) and cytogenetic/molecular risk group (right). (D and E) sCD27 serum levels (D) and Kaplan-Meier survival curves (E) of the different risk groups. (A, C, and D) Red lines indicate mean. (F–H) Kaplan-Meier survival curves for sCD27. (F) Favorable risk group (*n* = 34), sCD27 threshold 470 U/ml. (G) Intermediate risk group (*n* = 68), sCD27 threshold 586 U/ml. (H) Adverse risk group (*n* = 35), sCD27 threshold 714 U/ml. (I) Multivariate analysis for sCD27 adjusted for risk group, age, percentage of blasts in BM and blood, and leukocyte counts. Statistics: (A, C [right], and D) one-way ANOVA; (C, left) Student's *t* test; (B and E–H) log-rank test; and (I) multiple Cox regression. *, P < 0.05; **, P < 0.01; ***, P < 0.001. adv., adverse; CI, confidence interval; fav., favorable; int., intermediate; OS, overall survival.

ing signals that induce LSC expansion, either by blocking proliferation or by forcing differentiation via asymmetric cell division may lead to resolution of the disease (Horton and Huntly, 2012; Bajaj et al., 2015).

CD27, a costimulatory receptor of the TNF superfamily, is constitutively expressed on lymphocytes and HSPCs (Nolte et al., 2009; Schürch et al., 2012). CD70, its only ligand, is expressed on activated lymphocytes and dendritic cells but is undetectable in homeostasis (Nolte et al., 2009). During immune activation, CD70/CD27 signaling promotes lymphocyte expansion and survival and modulates hematopoiesis by regulating HSPCs (Nolte et al., 2005, 2009). Interestingly, CD70 is aberrantly expressed on different solid tumors and lymphomas and was shown to induce local immunosuppression in glioblastoma and renal cell carcinoma (Grewal, 2008; Nolte et al., 2009).

In this study, we demonstrate that AML blasts and AML stem/progenitor cells coexpress CD70 and CD27. Soluble CD27 (sCD27), a marker for the extent of CD70/CD27 interactions in vivo, is considerably increased in the sera of newly diagnosed AML patients and is a strong prognostic biomarker for poor overall survival independently of age or cytogenetic/molecular risk group. CD70/CD27 signaling in AML cells induces stem cell gene signature pathways including canonical Wnt, JAK/STAT, Hedgehog, and TGF-β signaling and promotes an undifferentiated and malignant state by increasing symmetric cell divisions. Blocking CD70/CD27 signaling promoted asymmetric cell divisions and differentiation of AML blasts, decreased growth and colony formation, and induced differentiation of AML stem/progenitor cells in vitro. In contrast, HSPCs from healthy BM donors were not affected by this treatment. Blocking CD70/CD27 signaling
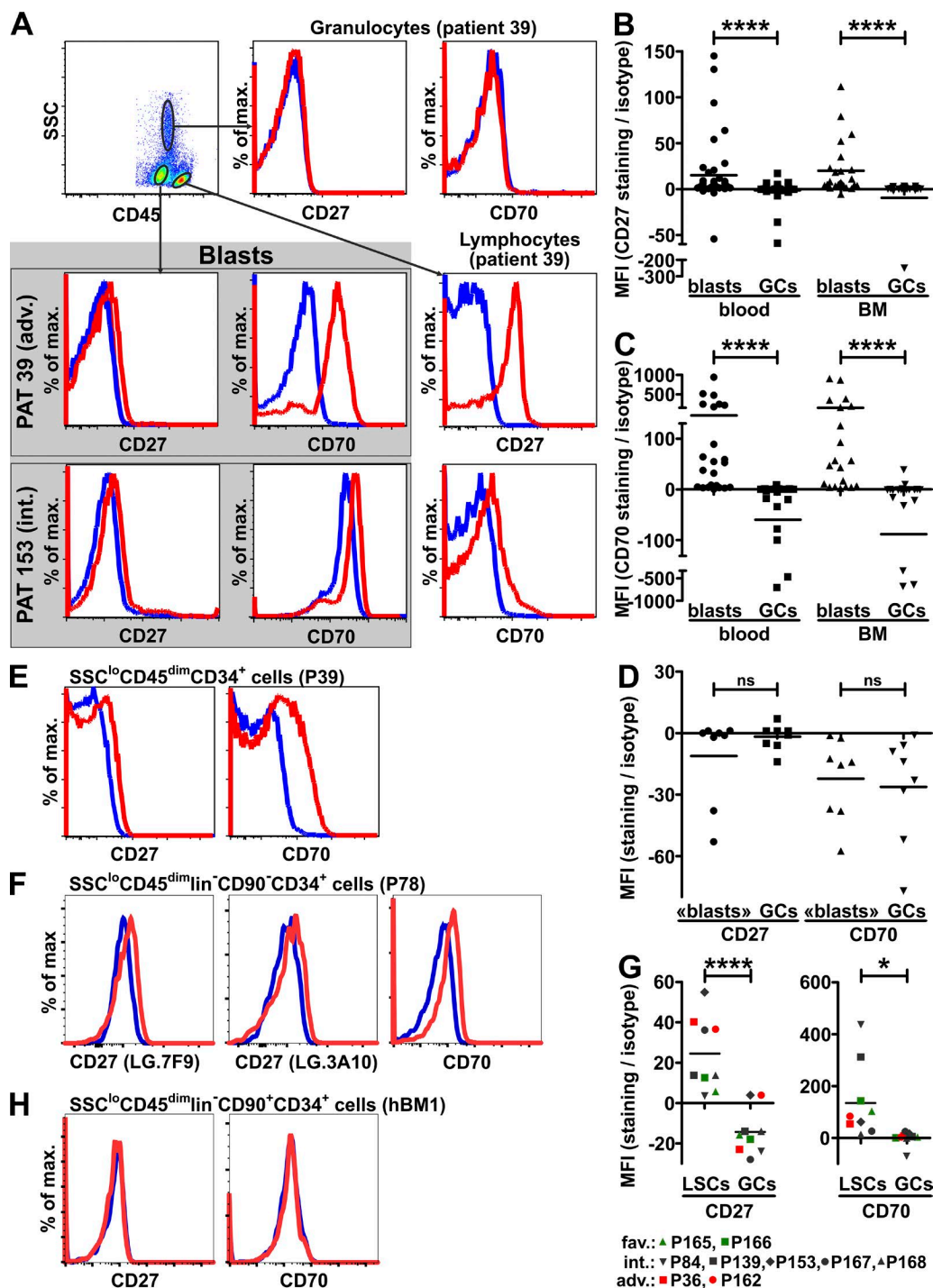
Figure 2. CD27 and CD70 are expressed on AML blasts and stem/progenitor cells. (A) Representative FACS plots of CD27 and CD70 stainings (red lines) and the respective isotype controls (blue lines) in freshly isolated blood from two newly diagnosed AML patients with a morphological frequency of ≥40% blasts (patient [PAT] 39, 62% blasts; and patient 153, 52% blasts). The gating strategy to identify granulocytes, blasts, and lymphocytes using CD45 and SSC is indicated. Histograms are representative for blood blasts of $n = 36$ (CD27) and $n = 22$ (CD70) positive patients. (B and C) Mean fluorescence intensity (MFI) quotients of CD27 (B) and CD70 stainings (C) versus the respective isotypes on blasts and granulocytes (GCs) from the blood and BM of newly diagnosed AML patients. CD27 stainings: $n = 42$ (blood) and $n = 25$ (BM). CD70 stainings: $n = 23$ (blood) and $n = 20$ (BM). Blood samples had a morphological frequency of ≥40% blasts, and BM samples had a blast infiltration of ≥40%, respectively. (D) MFI quotients of CD27 and CD70 versus the respective isotypes on cells in the CD45^{dim}SSC^{lo} gate (blasts) and GCs from the blood of healthy controls ($n = 8$). (E and F) CD27 and CD70 stainings (red lines) and the respective isotype controls (blue lines) on CD45^{dim}SSC^{lo}CD34$^+$ AML stem/progenitor cells from the BM of patient 39 (80% BM blasts; E) and CD45^{dim}SSC^{lo}
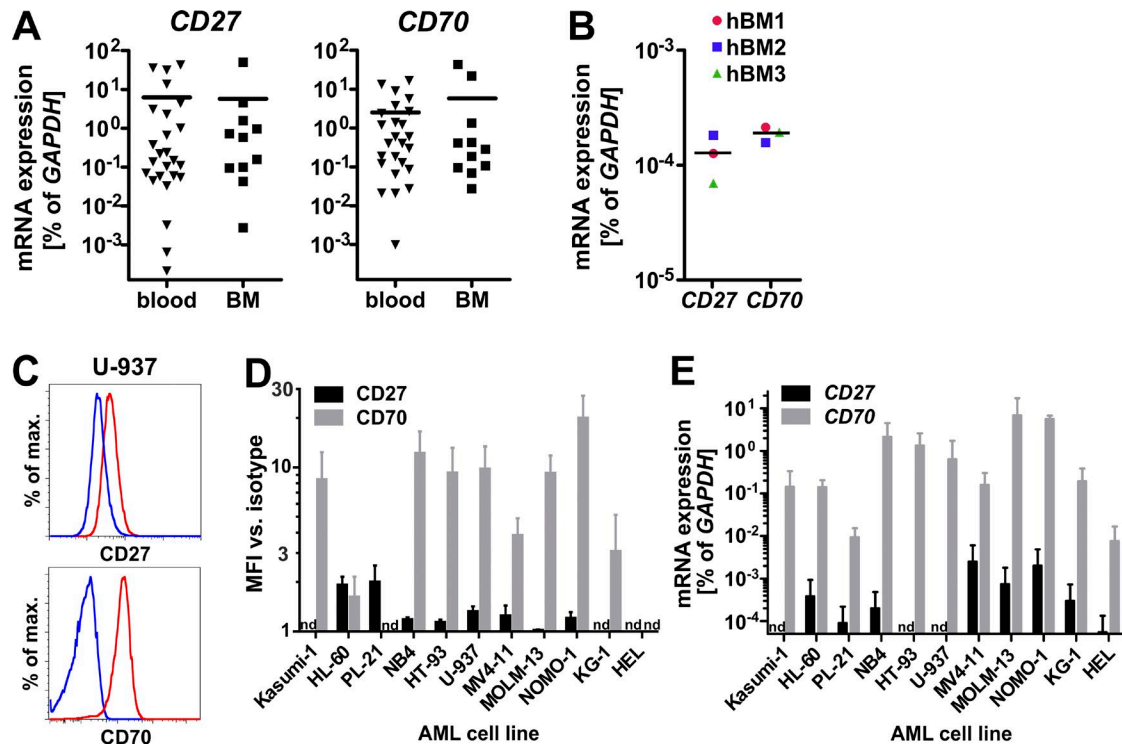
Figure 3. Expression of *CD27* and *CD70* in AML blasts, stem/progenitor cells from healthy BM donors, and AML cell lines. (A and B) Expression of *CD27* and *CD70* mRNA (qRT-PCR) in FACS-sorted CD45^{dim}SSC^{lo} AML blasts from blood (n = 26) and BM (n = 11) of newly diagnosed AML patients (A) and in FACS-sorted BM CD45^{dim}SSC^{lo}lin$^-$CD90$^+$CD34$^+$ HSPCs from healthy BM (hBM) donors (n = 3; B). (C) Expression of CD27 (red line, top) and CD70 (red line, bottom) versus the respective isotype controls (blue lines) in the AML cell line U-937. One representative histogram of five (CD27) and three (CD70) is shown. (D) Quotients of mean fluorescence intensity (MFI) of CD27 and CD70 expression versus the respective isotype in 11 different AML cell lines. Pooled data from n = 2–6 (CD27) and n = 2–5 (CD70) independent experiments are shown, respectively. (E) Expression of *CD27* and *CD70* mRNAs in 11 different AML cell lines (qRT-PCR). Pooled data from n = 2 (CD27) and n = 2–5 (CD70) independent experiments are shown. Data are shown as mean ± SEM. nd, not detected.

by mAb in murine AML xenografts delayed disease progression, reduced the number of AML stem/progenitor cells and prolonged survival.

RESULTS

sCD27 is increased in sera of AML patients and is an independent negative prognostic biomarker

CD70/CD27 signaling is deregulated in solid tumors, lymphoma, and CML (Grewal, 2008; Nolte et al., 2009; Schürch et al., 2012; Riether et al., 2015). To investigate a potential role of CD70/CD27 signaling in AML, we established a liquid biobank of sera and freshly isolated blood and BM samples from untreated AML patients at first diagnosis at our institution from 2011 to 2015. Because CD27 ligation results in the release of sCD27 by shedding, sCD27 can serve as a biomarker for the extent of CD70/CD27 interactions in vivo (Nolte et al., 2009). Overall, sCD27 serum levels were significantly increased in 137 AML patients compared with healthy controls (Fig. 1 A). To assess serum sCD27 in relation to overall survival, receiver operating characteristic curve analysis was performed in 30% of randomly selected patients. This resulted in an optimal threshold of 577 U/ml to define low and high. Using this threshold for the entire cohort, Kaplan-Meier analysis revealed that patients with low serum sCD27 (≤577 U/ml) survived significantly longer than patients with high serum sCD27 (Fig. 1 B).

Cytogenetic/molecular risk group and patient age are important established prognostic parameters in AML (Zeisig et al., 2012) and possibly acted as confounding factors in our analysis. Age and serum sCD27 levels did not

lin$^-$CD90$^-$CD34$^+$ AML stem/progenitor cells from the blood of patient 78 (72% blood blasts; F). In F, CD27 was stained with two different mAb clones. (G) MFI quotients of CD27 and CD70 versus the respective isotypes on blood CD45^{dim}SSC^{lo}lin$^-$CD90$^-$CD34$^+$ AML stem/progenitor cells (LSCs; n = 9). (B, C, D, and G) Horizontal lines indicate the mean. (H) CD27 and CD70 stainings (red lines) and the respective isotype controls (blue lines) on CD45^{dim}SSC^{lo}lin$^-$CD90$^+$CD34$^+$ HSPCs from one representative healthy BM donor of n = 3. See Fig. S1 (A and B) for details about the gating strategy used. Statistics: Mann–Whitney test. *, P < 0.05; ****, P < 0.0001. adv., adverse; fav., favorable; int., intermediate.

CD70/CD27 signaling promotes blast stemness in AML | Riether et al.
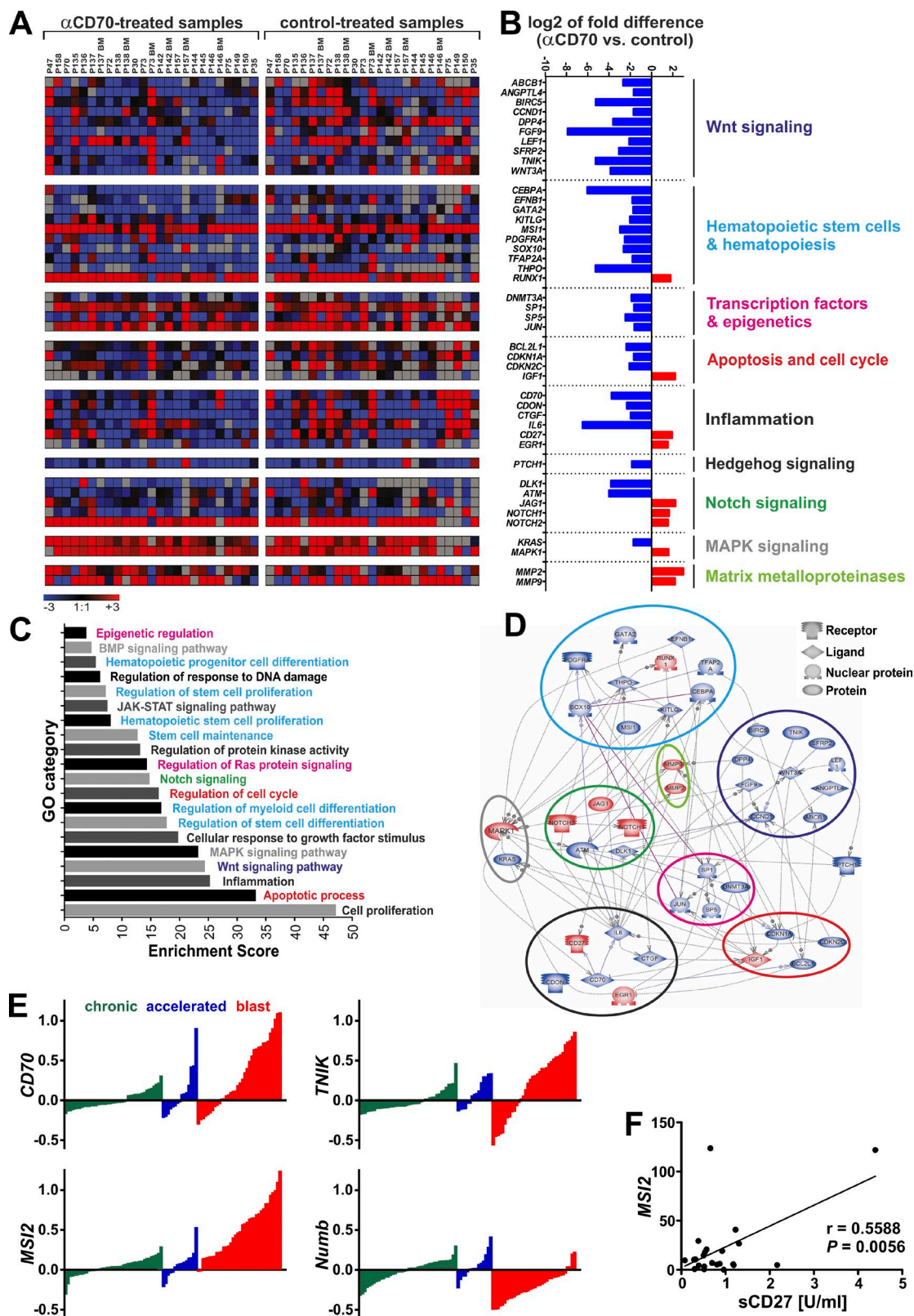
Figure 4. Stem cell gene expression and signaling pathways in AML and CML are linked to CD70/CD27 signaling. (A–D) Paired samples of 10^5 FACS-sorted CD45^dim SSC^lo CD33^+ AML blasts from the blood and BM of 20 different newly diagnosed patients (blood, *n* = 20; and BM, *n* = 6) were cultured in vitro for 72 h in the presence of blocking αCD70 or control mAb. (A) Heat map of differentially expressed genes in αCD70- versus control mAb–treated blasts.

significantly differ between patients in the favorable, intermediate, or adverse risk groups (Fig. 1, C and D; and Table S1). As expected, Kaplan-Meier survival curves revealed statistically significant survival differences between the different risk groups (Fig. 1 E). Furthermore, serum sCD27 demonstrated prognostic value in subgroup analyses within the different risk groups (Fig. 1, F–H). In addition, serum sCD27 correlated significantly with the percentage of blasts in BM (Table S1 and not depicted). Importantly, however, multivariate analysis for sCD27 levels adjusted for risk group, patient age, percentage of blasts in BM and blood, and leukocyte counts confirmed serum sCD27 as a strong independent prognostic marker in the entire AML patient cohort (Fig. 1 I).

In contrast, high *CD27* mRNA levels in two different publicly available AML microarray datasets (Valk et al., 2004; Metzeler et al., 2008) were associated with a favorable prognosis (unpublished data). However, these datasets were not generated using purified blasts but with total PBMCs containing immune cells such as lymphocytes that express substantially higher levels of CD27 than AML blasts (Fig. 2 A). In accordance, *CD27* mRNA levels positively correlated with *CD3*, *CD8*, and *CD4* mRNAs in these datasets (unpublished data). Therefore, high CD27 mRNA expression in AML PBMCs rather reflects an activated immune system that promotes survival and does not necessarily indicate the extent of CD27 signaling on AML blasts.

These results indicate that sCD27 in serum but not *CD27* mRNA in PBMCs is an independent negative prognostic biomarker for overall survival in AML.

AML blasts and stem/progenitor cells express the TNF superfamily ligand–receptor pair CD70/CD27

We next intended to test whether CD27 and/or CD70 protein can be detected on AML blasts by FACS. The CD45 and side scatter (SSC) gating strategy is an established method to identify blasts (CD45^{dim}SSC^{lo}) in phenotypically different AML patient samples, but the blast gate may include other cell populations (Borowitz et al., 1993; Kroft and Karandikar, 2007; Gorczyca, 2010). Accordingly, the blast gate can be identified in healthy individuals as well. We therefore only included patients in this analysis with a documented blast frequency of ≥40% as determined by morphology. Healthy donors served as negative controls. As expected, CD27 and CD70 were expressed on lymphocytes but not on granulocytes. Interestingly, CD27 and

CD70 were detectable on AML blasts as well (Fig. 2 A). CD27 was detected on blasts in 36/42 (86%) blood and 24/25 (96%) BM samples, whereas CD70 was detected in 22/23 (96%) blood and 20/20 (100%) BM samples (Fig. 2, B and C). CD27 and CD70 were similarly expressed on blasts in blood and BM (Fig. 2, B and C). Both proteins were detected on AML blasts in 16/23 (70%) blood and 19/20 (95%) BM samples (Table S1). In contrast, cells in the blast gate of healthy controls that mainly represent monocytes and basophils (Aoun and Pirruccello, 2007) did not express CD27 or CD70 (Fig. 2 D and Fig. S1 A). The AML stem/progenitor cell population that contains the disease-initiating LSCs in the majority of AML samples is a subfraction of CD45^{dim}SSC^{lo} blasts characterized as lineage (lin)$^-$CD90$^-$CD34$^+$ (Fig. S1 B; Blair et al., 1997; Bonnet and Dick, 1997; Sarry et al., 2011; Terwijn et al., 2014). Importantly, CD70 and CD27 were similarly detected on BM CD45^{dim}SSC^{lo}CD34$^+$ as well as blood CD45^{dim}SSC^{lo} lin$^-$CD90$^-$CD34$^+$ AML cells (Fig. 2, E–G), In contrast, BM HSPCs (CD45^{dim}SSC^{lo}lin$^-$CD90$^+$CD34$^+$ BM cells; Majeti et al., 2007) from patients who underwent BM biopsy for other reasons than leukemia (healthy BM donors) did not express CD70 or CD27 (Fig. 2 H).

Because CD27 ligation leads to shedding of the protein (Nolte et al., 2009), FACS analysis may underestimate its expression. Indeed, all FACS-sorted AML blasts expressed *CD27* and *CD70* mRNAs (Fig. 3 A). In addition, *CD27* and *CD70* mRNA expression in blasts from blood and BM was 10^3- to 10^5-fold higher than in HSPCs from healthy BM donors (Fig. 3 B). Furthermore, CD27 and CD70 were detected in the majority of AML cell lines analyzed (Fig. 3, C–E).

These results indicate that blasts and stem/progenitor cells of most AML patients as well as AML cell lines coexpress the TNF superfamily ligand–receptor pair CD70/CD27.

CD70/CD27 signaling induces stem cell signature and proliferation–promoting pathways in primary AML blasts

To investigate the possibility of cell-autonomous and/or paracrine CD70/CD27 signaling, we cultured FACS-sorted AML blasts from 20 different newly diagnosed patients in the presence of a blocking αCD70 mAb (clone 41D12-D; Silence et al., 2014; Riether et al., 2015) or a control mAb in vitro. sCD27 levels in cell supernatants were significantly lower in the presence of αCD70 as compared with control mAb, indicating that the CD70/CD27 interaction was

(B) Fluidigm-based gene expression profiles in signaling pathways regulated by the CD70/CD27 interaction. Log$_2$ fold differences of gene expression levels in αCD70- versus control mAb–treated blasts are shown. (C) Histogram of GO enrichment analysis of the biological pathways significantly affected in AML blasts treated with αCD70 mAb. (D) Gene network and canonical pathway analysis highlighting the regulation and interrelation of the most important CD70/CD27 interaction target genes in AML blasts. (E) A publicly available microarray dataset (GSE4170) that assessed gene expression profiles during progression of CML was analyzed for *CD70*, *TNIK*, *MSI2*, and *Numb* using the Gene Expression Omnibus GEO2R tool. Expression values of patients in chronic-phase (*n* = 42; green bars), accelerated-phase (*n* = 15; blue bars), and blast-phase (*n* = 36; red bars) CML are shown. (F) *MSI2* expression in control-treated blasts from A–D was correlated to the sCD27 level in supernatants. Statistics: Pearson *r*.
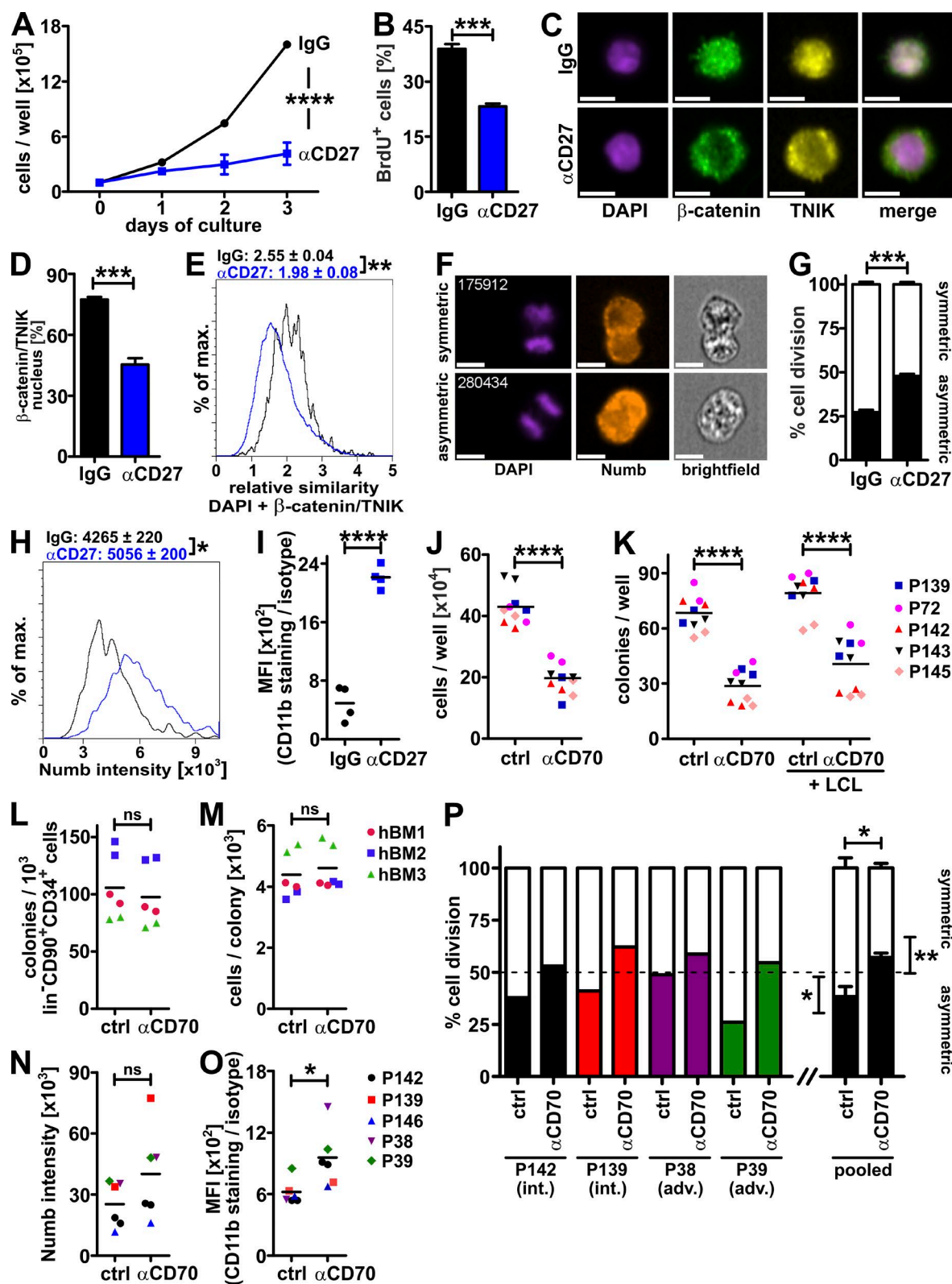
Figure 5. **CD70/CD27 signaling activates Wnt signaling in AML cells and promotes symmetric cell division.** (A–I) 10^5 U-937 cells were cultured in the presence of 10 µg/ml blocking αCD27 mAb or control IgG for 3 d. (A) Live cell numbers. One representative experiment of three, each run in duplicates, is shown. (B) BrdU incorporation on day 3 (FACS). Pooled data ($n = 3$) from two independent experiments are shown. (C) Intracellular localization of active β-cat-

efficiently blocked (αCD70: 4.39 ± 0.20 U/ml; control: 3.25 ± 0.13 U/ml; P < 0.0001). We next quantified the expression of 91 different stem cell signature and proliferation-promoting genes important in hematopoiesis using Fluidigm dynamic array (Table S2). 45 genes were differentially expressed in αCD70 compared with control mAb–treated blasts (Fig. 4 A). Hierarchical clustering revealed that blocking CD70/CD27 signaling down-regulated numerous target genes of the canonical Wnt pathway, which is essential for leukemogenesis (Fig. 4 B; Staal and Clevers, 2005). Moreover, the expression of important HSC and hematopoiesis genes, transcription factors, epigenetic modifiers, apoptosis, and cell cycle regulators as well as inflammatory and Hedgehog-signaling genes was reduced. Of note, blocking CD27 signaling reduced important stem cell genes such as *Musashi* and the *TNF receptor associated factor 2 (TRAF2)*– and *NCK-interacting kinase* (*TNIK*; Mahmoudi et al., 2009; Ito et al., 2010). In contrast, some genes related to Notch signaling, MAPK signaling, and matrix metalloproteinases were up-regulated upon blocking CD70/CD27 signaling (Fig. 4 B). Gene ontology (GO) enrichment analysis of the differently expressed genes revealed 20 different GO categories that were significantly regulated (over threefold) and established a hierarchy of pathways with cell proliferation, apoptosis, inflammation, and Wnt and MAPK signaling at the top of the hierarchy (Fig. 4 C). Furthermore, gene networks and canonical pathways within the 45 genes regulated by CD70/CD27 signaling were analyzed in silico using direct force analysis to study possible protein–protein and/or genetic interactions. This analysis revealed that stemness-associated genes that were down-regulated by blocking CD70/CD27signaling are directly triggered by Wnt pathway–associated genes (Fig. 4 D).

Therefore, CD70/CD27 signaling induces a stem cell signature at least partially via Wnt signaling, leading to a more undifferentiated and malignant state. Because disease evolution could not be tested in primary AML samples, we analyzed the expression of genes involved in the CD70/CD27 signaling pathway during the evolution of indolent chronic-phase CML via accelerated-phase to blast-phase CML, a fatal acute leukemia. Using a publicly available microarray dataset (Radich et al., 2006), we found a continuous increase in *CD70* and *TNIK* expression from chronic- to accelerated- to blast-phase CML. In line with Ito et al. (2010), *Musashi* expression increased, whereas expression of the cell-fate determinant *Numb* decreased during CML progression (Fig. 4 E). Correspondingly, sCD27 levels in supernatants of control-treated AML blasts correlated with *Musashi* expression (Fig. 4 F). These data indicate that CD70/CD27 signaling is associated with the expression of stem cell genes such as *Musashi* and *TNIK* and disease progression in myeloid leukemia.

CD70/CD27 signaling regulates the cell fate of AML cells by activating the canonical Wnt pathway

U-937 cells express CD27 and CD70 as analyzed by FACS (Fig. 3 C). To functionally investigate the pathways that resulted from the array analysis, we treated U-937 cells with blocking αCD27 or αCD70 mAb. This strongly inhibited cell proliferation, leading to reduced cell numbers after 3 d of culture (Fig. 5, A and B; and not depicted). To further investigate the effect of CD27 signaling on the Wnt pathway, we first determined the cellular localization of β-catenin, the key molecule of canonical Wnt signaling (Clevers and Nusse, 2012). ImageStream[X] analysis showed nuclear translocation of active β-catenin in control-treated U-937 cells, whereas blocking CD27 resulted in preferential cytoplasmic β-catenin localization (Fig. 5, C and D). This indicates that CD27 signaling activates the Wnt pathway and confirms the GO analysis of primary AML blasts. TNIK, an essential activator of Wnt target genes (Mahmoudi et al., 2009), colocalized with β-catenin (Fig. 5, C and D). Confirmative, similarity analysis using IDEAS software (George et al., 2006) revealed significantly less nuclear colocalization of β-catenin/TNIK in αCD27- versus control-treated cells (Fig. 5 E). This correlated with significantly reduced relative luminescence units (RLU) in a T cell transcription factor (TCF)/lymphoid enhancer binding factor (LEF) luciferase Wnt signaling reporter assay (αCD27: 1,458 ± 32 RLU; control: 616 ± 24 RLU; P = 0.0052) and reduced transcription of the Wnt target genes *BIRC5*, *CCND1*, *LEF*, *MYC*, and *VEGF* (unpublished data).

enin and TNIK (ImageStream[X]). One representative image of *n* = 17,000 (αCD27) and *n* = 11,000 (IgG) cells is shown, respectively. (D) Percentage of cells with nuclear colocalization of active β-catenin/TNIK. (E) Relative similarity of DAPI and active β-catenin/TNIK. (F–H) Distribution and intensity of Numb expression in dividing U-937 cells (ImageStream[X]). (F) Representative examples for asymmetric and symmetric cell division. (G) Percentage of asymmetric and symmetric cell divisions in IgG- versus αCD27-treated U-937 cells (one experiment run in triplicates; analysis of *n* = 353–375 dividing cells per condition). (H and I) Numb intensity (ImageStream[X]; H) and CD11b expression (FACS) in the total U-937 cell population (I). Pooled data from two independent experiments run in duplicates. (J and K) FACS-sorted CD45^{dim}SSC^{lo} blasts from the blood of *n* = 5 different newly diagnosed AML patients were cultured in duplicates in the presence of 10 µg/ml αCD70 or control mAb. (J) Cells per well after 7 d (liquid culture, start: 10[5] cells). (K) Colonies per well after 2 wk (methylcellulose, start: 10[3] cells), with or without overnight pre-incubation with 10[5] irradiated (10 Gy) cells of a CD70-expressing LCL. (L and M) 10[3] FACS-sorted CD45^{dim}SSC^{lo}lin^{−}CD90^{+}CD34^{+} BM stem/progenitor cells from *n* = 3 different healthy BM (hBM) donors were cultured in duplicates in methylcellulose in the presence of 10 µg/ml αCD70 or control mAb. Colonies (L) and cells per well (M) were enumerated after 2 wk. (N–P) 10[5] FACS-sorted CD45^{dim}SSC^{lo} blasts from the blood of *n* = 5 different newly diagnosed AML patients were cultured in liquid culture for 7 d in the presence of 10 µg/ml αCD70 or control mAb. Numb intensity (ImageStream[X]; N), expression of CD11b (FACS; O), and percentage (P) of asymmetric and symmetric cell divisions in the total cell population (analysis of *n* = 61–201 dividing cells per condition per patient sample). Data are shown as mean ± SEM. Statistics: (A) two-way ANOVA; (B, D, E, G–J, and L–P) *t* test; and (K) one-way ANOVA. *, P < 0.05; **, P < 0.01; ***, P < 0.001; ****, P < 0.0001. Bars, 10 µm. adv., adverse; ctrl, control; int., intermediate; MFI, mean fluorescence intensity.
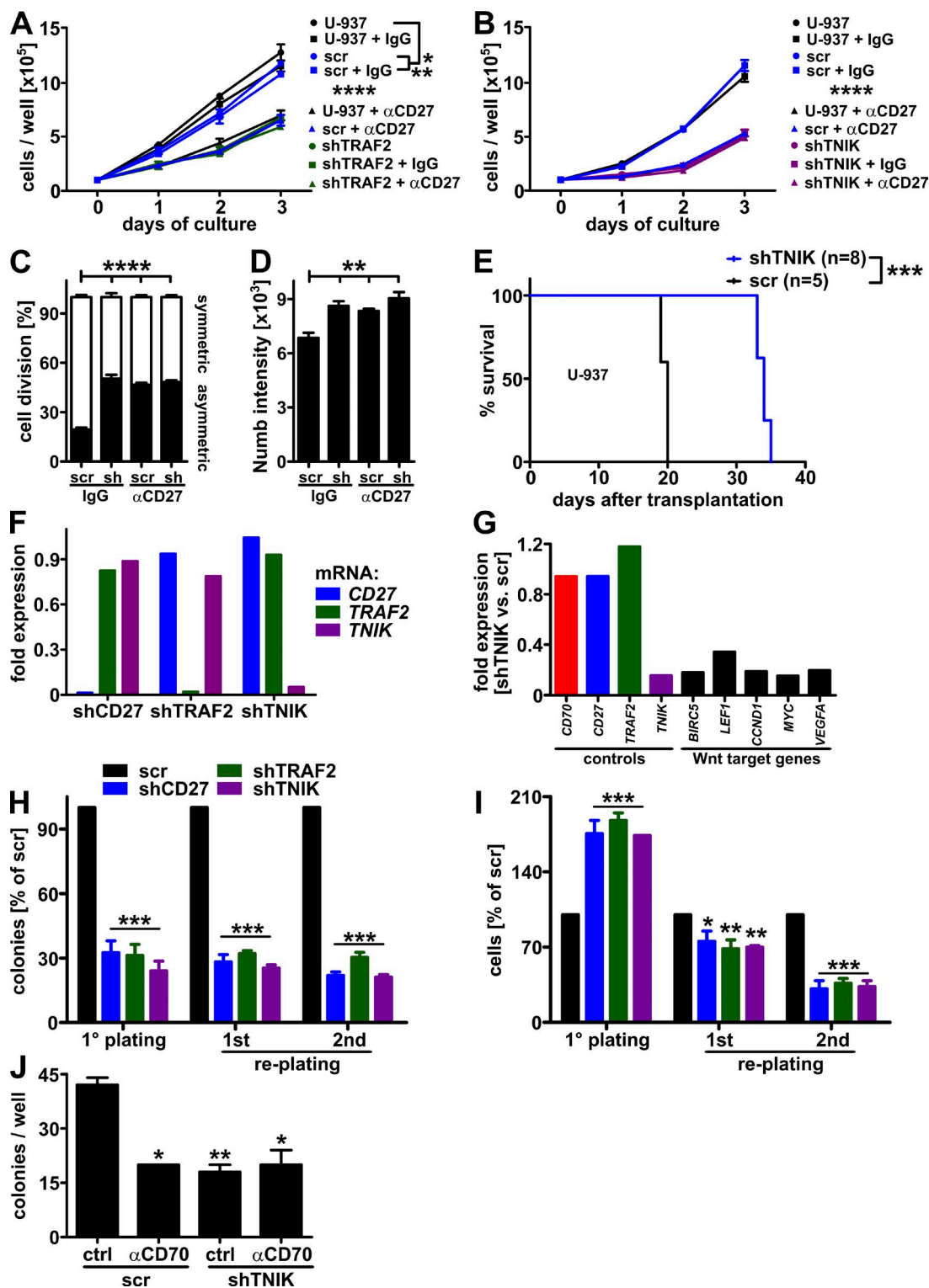
Figure 6. **The CD70/CD27 interaction activates Wnt signaling in AML cells via TRAF2 and TNIK.** (A and B) 10^5 U-937 cells stably expressing shRNA against TRAF2 (shTRAF2; A) or TNIK (shTNIK; B) were cultured in duplicates with 10 µg/ml blocking αCD27 mAb or control IgG for 3 d. Untreated and scrRNA-expressing cells were used as controls. Live cells were enumerated daily. (B) One representative of two independent experiments is shown. (C and D) 10^5 scr- and shTNIK-transduced U-937 cells were cultured in triplicates in the presence of IgG or αCD27 mAb. Percentage of asymmetric and symmetric cell divisions (analysis of $n = 84–161$ dividing cells per condition; C) and Numb intensity in the total cell population (D) are shown. (E) Kaplan-Meier survival curves of NSG mice xenotransplanted i.v. with 10^5 scr- or shTNIK-transduced U-937 cells. (F–J) CD27 (shCD27), TRAF2, or TNIK were stably knocked down

Interestingly, blocking the CD70/CD27 interaction resulted in a higher percentage of asymmetrically dividing U-937 cells, as analyzed by the intracellular distribution of the cell-fate determinant Numb (Fig. 5, F and G; Wu et al., 2007; Ito et al., 2010; Zimdahl et al., 2014). As a consequence, blocking CD70/CD27 signaling resulted in increased amounts of intracellular Numb and surface CD11b (Fig. 5, H and I), indicating cell differentiation.

In FACS-sorted blasts from different AML patients, αCD70 treatment resulted in significantly reduced cell numbers in liquid cultures (Fig. 5 J) and colony formation in methylcellulose (Fig. 5 K), confirming the results observed in U-937 cells. Moreover, preincubation of AML blasts with an irradiated CD70-expressing lymphoblastoid B cell line (LCL; Ochsenbein et al., 2004) did not significantly increase colony formation, suggesting that CD70/CD27 interactions in AML blasts are already maximal (Fig. 5 K). In contrast and in line with our previous work (Riether et al., 2015), αCD70 treatment did not affect colony formation of HSPCs from healthy BM donors (Fig. 5, L and M). We observed elevated Numb protein levels and a significantly increased expression of the differentiation marker CD11b in AML blasts after αCD70 treatment, whereas CD14 and CD33 expression remained unchanged (Fig. 5, N and O; and not depicted). Control-treated blasts divided significantly more often symmetrically than asymmetrically. Blocking CD70 reversed this balance in all patient samples and significantly increased asymmetric over symmetric cell divisions (Fig. 5 P).

Together, these results indicate that the CD70/CD27 interaction in AML blasts promotes symmetric cell division, resulting in more undifferentiated stem-like cells.

CD27 signaling regulates cell fate decision via TRAF2 and TNIK

To investigate whether CD27 signaling regulates AML cell fate via TRAF2 and TNIK (Schürch et al., 2012), we knocked down these CD27 downstream molecules in U-937 cells using shRNA. TRAF2 or TNIK knockdown reduced U-937 cell growth to a similar extent as αCD27 treatment. Interestingly, αCD27 treatment of TRAF2 or TNIK knockdown cells did not further decrease cell growth (Fig. 6, A and B). Similarly to blocking CD27 signaling (Fig. 5, G and H), TNIK knockdown promoted asymmetric cell division and increased Numb expression in the U-937 cell population, which could not be further enhanced by adding αCD27 mAb (Fig. 6, C and D). Moreover, stable knockdown of TNIK in U-937 cells

significantly prolonged survival of xenotransplanted NOD/LtSz-*scid* IL-2Rγ[null] (NSG) mice (Fig. 6 E). This suggests that CD27 signaling increases symmetric AML cell division via TRAF2/TNIK signaling.

To further elaborate on these findings in a more physiological setting, we knocked down CD27, TRAF2, or TNIK in primary AML blasts. Knockdown efficiency and specificity were assessed on mRNA and protein level by quantitative real-time PCR (qRT-PCR) and ImageStream[X] analysis, respectively (Fig. 6 F and not depicted). TNIK knockdown decreased Wnt target gene expression (Fig. 6 G), and CD27, TRAF2, or TNIK knockdowns reduced colony formation in methylcellulose (Fig. 6 H). Importantly, this reduction was similar between blasts with CD27, TRAF2, or TNIK knockdown and was maintained during serial replating. In contrast, cell numbers per well were considerably increased in knockdown cells during the first round of plating but significantly declined in further rounds, indicating that CD27, TRAF2, or TNIK knockdown induced differentiation, repressed self-renewal, and led to exhaustion of these cells (Fig. 6 I). As expected, the addition of αCD70 mAb to TNIK knockdown AML blasts did not further reduce colony formation (Fig. 6 J).

These results indicate that Wnt-activating and stemness-maintaining CD27 signals are mainly mediated via TRAF2 and TNIK in AML cells.

Blocking the CD70/CD27 interaction in AML stem/progenitor cells inhibits cell growth and colony formation and induces differentiation

FACS-sorted CD45^{dim}SSC^{lo}lin^{−}CD90^{−}CD34^{+} AML stem/progenitor cells from blood of six patients from different cytogenetic/molecular risk groups were cultured in the presence of blocking αCD70 or control mAb. After 3 d, cells were enumerated, and sCD27 levels were determined in supernatants. Blocking CD70 significantly reduced cell numbers per well and sCD27 levels in supernatants (Fig. 7, A and B). Importantly, sCD27 levels were also reduced when adjusted for different cell numbers (Fig. 7 C). To assess colony-forming capacity, AML stem/progenitor cells were cultured in methylcellulose in the presence of blocking αCD70 or control mAb. In line with our results from blasts (Fig. 6 J), αCD70 treatment significantly reduced colony formation from AML stem/progenitor cells (Fig. 7 D). Serial replating experiments revealed that this effect was maintained even in the absence of αCD70 mAb in the primary or secondary replating cul-

in FACS-sorted CD45^{dim}SSC^{lo} blasts from the blood of patient 142. Scr-transduced blasts were used as controls. (F) Knockdown efficiency and specificity were assessed by quantifying *CD27*, *TRAF2*, and *TNIK* mRNA (qRT-PCR). Data are shown as fold expression of scr (=1). (G) Wnt target gene expression after TNIK knockdown (qRT-PCR). (H and I) Duplicates of 10^3 shCD27, shTRAF2, shTNIK, and scr blasts were cultured in methylcellulose, and colonies (H) and cells per well (I) were enumerated after 2 wk (1° plating). 5×10^3 cells were then replated, and colonies and cells were assessed 2 wk later (first replating). This was repeated one more time (second replating). (H and I) Percentages of knockdown versus scr blasts are shown. (J) Duplicates of 10^3 shTNIK and scr blasts were cultured in methylcellulose in the presence of 10 µg/ml αCD70 or control mAb, and colonies were enumerated after 2 wk. Data are shown as mean ± SEM. Statistics: (A, B, H, and I) two-way ANOVA; (C, D, and J) one-way ANOVA; and (E) log-rank test. *, P < 0.05; **, P < 0.01; ***, P < 0.001; ****, P < 0.0001.
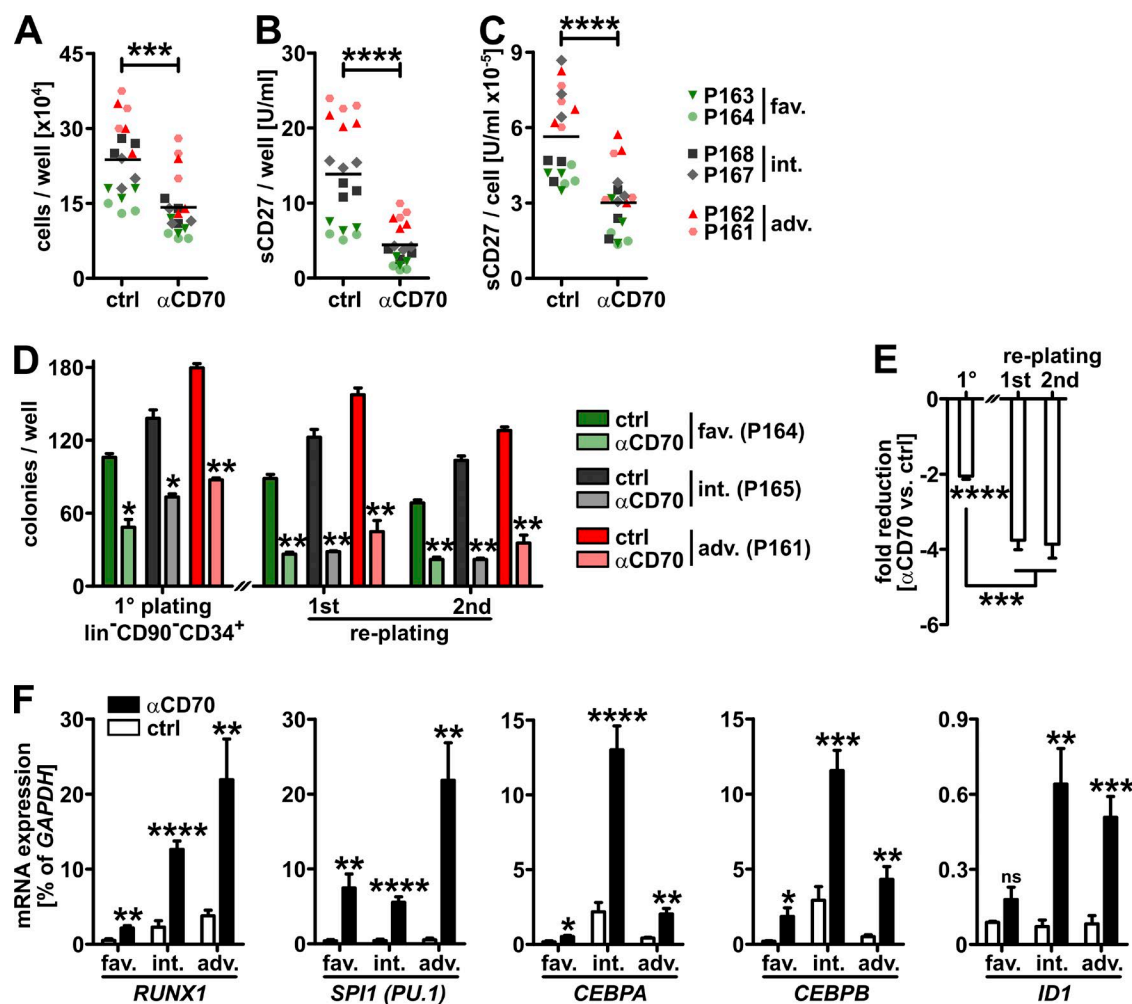
Figure 7. Blocking the CD70/CD27 interaction in AML stem/progenitor cells inhibits cell growth and colony formation and induces differentiation. (A–C) Duplicates of 10^5 FACS-sorted CD45^{dim}SSC^{lo}lin$^-$CD90$^-$CD34$^+$ stem/progenitor cells from blood of six different AML patients were cultured in liquid culture in the presence of 10 µg/ml αCD70 or control mAb for 3 d. (A and B) Cell numbers per well (A) and sCD27 levels (B) in supernatants were determined. (C) Levels of sCD27 per live cell after 3 d of culture were calculated. (D and E) 10^3 FACS-sorted CD45^{dim}SSC^{lo}lin$^-$CD90$^-$CD34$^+$ stem/progenitor cells from blood of three different AML patients were cultured in duplicates overnight in liquid medium in 96-well plates in the presence of 10 µg/ml αCD70 or control mAb. Cells were then plated into methylcellulose in the presence of 10 µg/ml αCD70 or control mAb for 2 wk (1° plating). 10^4 cells were then replated into methylcellulose without mAbs, and colonies and cell numbers were assessed 2 wk later (first replating). This was repeated one more time (second replating). (E) Fold reduction of colony formation by αCD70 mAb in primary plating and replating (pooled data from D). (F) 10^5 FACS-sorted CD45^{dim}SSC^{lo}lin$^-$CD90$^-$CD34$^+$ AML stem/progenitor cells from the patients from A–C were cultured overnight in liquid culture in the presence of 10 µg/ml αCD70 or control mAb, and the expression of *RUNX1*, *CEBPA*, *CEBPB*, *SPI1* (*PU.1*), and *ID1* mRNA was analyzed (qRT-PCR, pooled data from two independent experiments). Data are shown as mean ± SEM. Statistics: (A–D and F) Student's *t* test; (E) one-sample Student's *t* test (1°) and one-way ANOVA (1° vs. first/second replating). *, P < 0.05; **, P < 0.01; ***, P < 0.001; ****, P < 0.0001. adv., adverse; ctrl, control; fav., favorable; int., intermediate.

tures (Fig. 7, D and E). In addition, the expression of the differentiation-inducing genes *RUNX1*, *SPI1* (*PU.1*), *CEBPα*, *CEBPβ*, and *ID1* (Rosenbauer and Tenen, 2007) was significantly increased in AML stem/progenitor cells cultured overnight in the presence of blocking αCD70 compared with control mAb (Fig. 7 F).

These findings indicate that blocking the CD70/CD27 interaction reduces AML stem/progenitor cell numbers and induces differentiation.

Blocking the CD70/CD27 interaction prolongs survival in AML xenotransplantation models

U-937 cells or FACS-sorted blasts from two different AML patients were injected i.v. into sublethally irradiated NSG mice. After 7 d of engraftment, NSG mice were randomized to αCD70 or control mAb treatment. αCD70 treatment significantly prolonged survival in xenotransplanted mice (Fig. 8, A–C). Similarly, stable TNIK knockdown in AML blasts prolonged survival of xenotransplanted mice (Fig. 8 D).
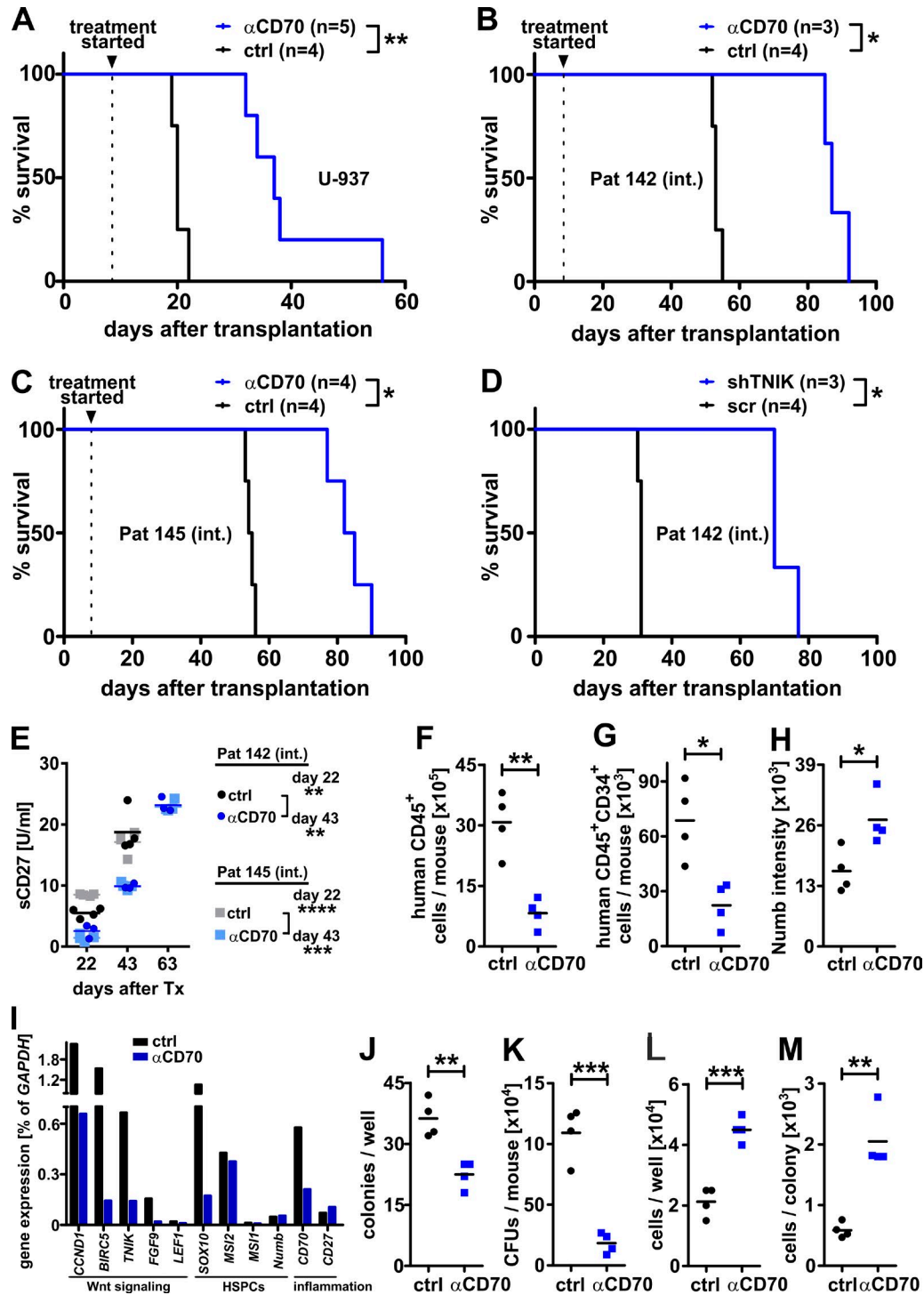
Figure 8. **Blocking CD70 promotes differentiation of xenotransplanted AML blasts and prolongs survival.** (A–C) Kaplan-Meier survival curves of NSG mice xenotransplanted i.v. with 10^5 U-937 cells (A) or 10^6 FACS-sorted CD45^{dim}SSC^{lo} blasts (B and C) from the blood of patients (Pat) 142 and 145, respectively. Mice were treated with 10 mg/kg αCD70 or control (ctrl) mAb every third day starting 7 d after transplantation. (D) Kaplan-Meier survival curves of NSG mice xenotransplanted i.v. with 10^6 FACS-sorted CD45^{dim}SSC^{lo} blasts from patient 142. Before transplantation, stable knockdown of TNIK was established. Scr-transduced cells were used as controls. (E) sCD27 was quantified in the serum of NSG mice from B and C at different time points. (F and G) 10^6 FACS-sorted CD45^{dim}SSC^{lo} blasts from patient 142 were xenotransplanted into NSG mice. Mice were treated as described for A–C. 40 d after transplantation, mice were sacrificed, and total numbers of human CD45$^+$ AML cells (F) and CD45$^+$CD34$^+$ AML stem/progenitor cells (G) in the BM were quantified (FACS). (H–M) Human CD45$^+$CD34$^+$ AML stem/progenitor cells were purified by FACS sorting. Numb intensity was analyzed by ImageStream^X (H),

Human sCD27 was present in the sera of NSG mice xenografted with primary AML samples, and its levels increased as the disease progressed. Interestingly, in αCD70-treated mice, human sCD27 levels were significantly lower than in controls, indicating that CD70 blockade specifically reduced CD27 signaling on human AML blasts in these mice (Fig. 8 E). αCD70 treatment significantly reduced total human CD45+ cells and CD45+CD34+ AML stem/progenitor cells in xenografted mice 40 d after transplantation (Fig. 8, F and G). Importantly, Numb expression was increased in the population of CD45+CD34+ AML stem/progenitor cells, indicating a more differentiated state (Fig. 8 H). Furthermore, FACS-sorted CD45+CD34+ AML stem/progenitor cells from αCD70-treated xenografted mice down-regulated the expression of several Wnt signaling–, hematopoiesis-, and inflammation–associated genes (Fig. 8 I) and formed significantly fewer colonies in methylcellulose per well than controls (Fig. 8 J). Similarly, the CFUs of sorted CD45+CD34+ AML stem/progenitor cells per mouse were significantly reduced by αCD70 treatment (Fig. 8 K). In contrast, cell numbers per well and per colony were considerably increased (Fig. 8, L and M).

Together, these data suggest that αCD70 treatment of xenografted mice prolonged survival by inducing differentiation of AML stem/progenitor cells.

Blocking the CD70/CD27 interaction reduces stem cell gene expression, induces differentiation, and inhibits self–renewal in AML stem/progenitor cells

To confirm and extend these findings, we performed xenografts with additional patient samples from each risk group. Two weeks after transplantation, NSG mice were randomized and treated for 2 wk with αCD70 or control mAb. αCD70 treatment did not affect total BM cell numbers (Fig. 9 A). In contrast, human CD45dimSSClo blasts and CD45dimSSClo lin−CD90−CD34+ AML stem/progenitor cells in BM were significantly reduced, irrespective of the cytogenetic/molecular risk group of the transplant (Fig. 9, B–D). Importantly, αCD70 treatment induced a significant up-regulation of CD27 on CD45dimSSClolin−CD90−CD34+ AML stem/progenitor cells (Fig. 9 E). In addition, αCD70 treatment resulted in a trend of CD11b and Numb up-regulation in human CD45dimSSClo AML blasts from xenografts (Fig. 9, F and G). Furthermore, FACS-sorted CD45dimSSClolin−CD90−CD34+ AML stem/progenitor cells from αCD70-treated mice formed significantly fewer colonies in methylcellulose per well than controls (Fig. 9 H). In contrast, cell numbers per colony were considerably increased (Fig. 9 I). Importantly, Fluidigm dynamic array analysis of ex vivo FACS-sorted human CD45dimSSClolin−CD90−CD34+ AML stem/pro-

genitor cells from xenografts revealed that αCD70 treatment resulted in a down-regulation of important stem cell– and hematopoiesis–associated genes (Fig. 9, J and K), confirming and extending our in vitro data from AML blasts (Fig. 4, A and B).

To confirm the reduction of AML stem/progenitor cell numbers in vivo, we performed secondary transplantations using whole BM cells from primary xenotransplanted NSG mice. NSG mice receiving BM cells from αCD70-treated primary xenografts survived significantly longer than NSG mice transplanted with BM cells from control mAb–treated primary xenografts (Fig. 10, A–D). Importantly, this effect was found in samples from all different cytogenetic/molecular risk groups.

These results indicate that blocking CD70/CD27 signaling reduces numbers and function and induces differentiation of AML stem/progenitor cells by inhibiting stem cell gene expression programs.

DISCUSSION

An undifferentiated malignant state is a hallmark of AML blasts that is maintained by cell-intrinsic signals, but also possibly regulated by cell–extrinsic cues (Bajaj et al., 2015). In this study, we document an unexpected role for the CD70/CD27 ligand–receptor pair in the induction of Wnt signaling and stem cell gene signatures in AML. To our knowledge, this is the first report showing that the interaction of a TNF super-family ligand–receptor pair induces stemness in cancer cells.

First, we focused on cells in the CD45dimSSClo gate that identifies blasts in different AML types (Borowitz et al., 1993; Kroft and Karandikar, 2007; Gorczyca, 2010). Using sensitive xenograft assays, Sarry et al. (2011) have identified heterogeneous AML LSCs in bulk leukemia samples in fractions different from the originally reported lin−CD34+CD38− population, even in cells expressing differentiation markers (Bonnet and Dick, 1997). Because stem cell gene signature profiles have been documented in bulk blast populations in AML (Gentles et al., 2010; Eppert et al., 2011), it has been suggested that differentiated blasts may exhibit plasticity and reenter the LSC state (Kreso and Dick, 2014). We then extended our analyses to lin−CD90−CD34+ cells, a subfraction of CD45dimSSClo cells that contains the disease-initiating LSCs in the majority of AML samples (Blair et al., 1997; Terwijn et al., 2014). Importantly, CD70/CD27 signaling induced stemness in AML blasts and in phenotypically defined stem/progenitor cells.

Stem cells can self-renew either by symmetric renewal leading to an expansion of the stem cell pool or by asymmetric division, by which the pool remains constant (Wu et al., 2007). Stem cell gene signatures predict therapy resistance

the expression of selected Wnt signaling and HSC genes were quantified by qRT-PCR (I), and 10³ cells were plated into methylcellulose for colony analysis (J–M). Colonies of human CD45+CD34+ AML stem/progenitor cells per well were enumerated (J), and total CFUs per mouse were calculated (K). Cells per well were enumerated (L), and cells per colony were calculated (M). Statistics: (A–D) log-rank test; (E–H and J–M) Student's *t* test. *, P < 0.05; **, P < 0.01; ***, P < 0.001; ****, P < 0.0001. int., intermediate.
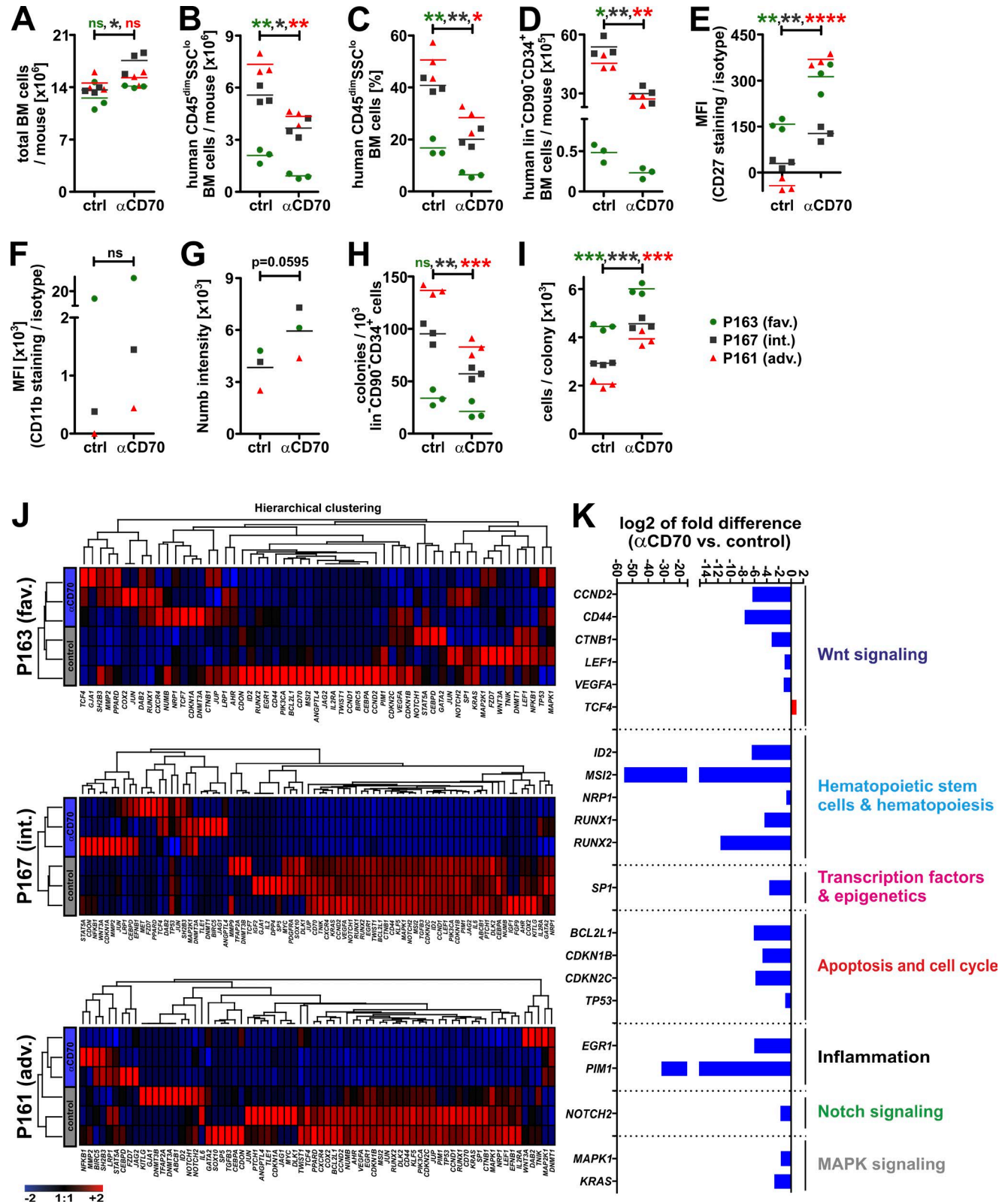
Figure 9. **Blocking the CD70/CD27 interaction inhibits stem cell gene expression and induces differentiation in AML stem/progenitor cells.** 10^6 FACS-sorted CD45^{dim}SSC^{lo} blasts from the blood of three different AML patients were injected i.v. into NSG mice (n = 3 mice per risk group per condition). After 2 wk of engraftment, mice were randomized and treated with 10 mg/kg αCD70 or control (ctrl) mAb every third day for 2 wk. (A–D) Total BM cell
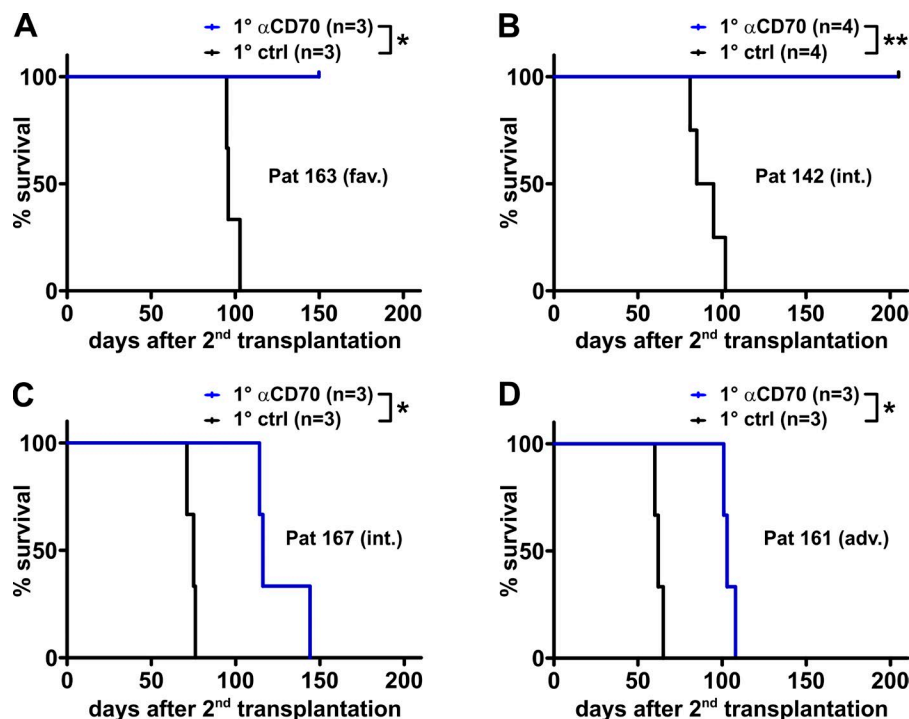
Figure 10. **Blocking the CD70/CD27 interaction in primary xenografts prolongs survival in secondarily transplanted NSG mice.** (A–D) Primary xenotransplants were established by i.v. injection of 10^6 FACS-sorted CD45^{dim}SSC^{lo} blasts from the blood of patients (Pat) 142, 161, 163, and 167, respectively, into NSG mice. After engraftment, mice were treated with 10 mg/kg αCD70 or control (ctrl) mAb every third day. Treatment was started 2 wk after transplantation, and mice were treated for 2 wk (A, C, and D) or started 7 d after transplantation (B), and mice were treated for 33 d. Then, 5×10^6 (A, C, and D) or 10^7 whole BM cells (B) from primary animals were injected i.v. into secondary NSG mice. Secondary recipients were left untreated, and Kaplan-Meier survival curves are shown. (A) Patient 163, favorable (fav.) risk group. (B and C) Patients 142 and 165, intermediate (int.) risk group, respectively. (D) Patient 161, adverse (adv.) risk group. Statistics: log-rank test. *, $P < 0.05$; **, $P < 0.01$.

and aggressive disease and negatively correlate with survival in AML and other malignancies (Ben-Porath et al., 2008; Gentles et al., 2010; Eppert et al., 2011; Metzeler et al., 2013). Mechanistically, stem cell determinants such as stemness-associated genetic signatures (Gentles et al., 2010; Eppert et al., 2011; Metzeler et al., 2013) and epigenetic profiles (Figueroa et al., 2010; Bartholdy et al., 2014) often oppose differentiation-inducing programs in AML blasts, leading to a block in terminal differentiation and senescence (Tenen, 2003). Currently, all-trans retinoic acid is the only approved drug that induces differentiation in blasts of acute promyelocytic leukemia (Grimwade et al., 2010), but other differentiation-inducing agents for AML are under investigation (Nowak et al., 2009). We now show that blocking the CD70/CD27 interaction shifted the balance from symmetric self-renewal to asymmetric cell division. This reduced the pool of AML stem/progenitor cells, leading to more differentiated leukemia cells, as documented by increased expression of the cell fate determinant Numb and the differentiation marker CD11b.

The canonical Wnt pathway, which is central for HSC development and maintenance, is constitutively active in myeloid leukemia and of crucial importance for LSCs (Staal and Clevers, 2005; Wang et al., 2010; Heidel et al., 2012). Self-renewal and β-catenin signatures in murine and human AML LSCs are often induced by translocations involving the mixed lineage leukemia gene family (Krivtsov and Armstrong, 2007). In our study, the CD70/CD27 interaction activated Wnt signaling in AML cells. However, CD70/CD27 signaling triggers additional survival-inducing and proliferation-promoting pathways, such as the canonical and noncanonical NF-κB pathways and the JNK pathway (Nolte et al., 2009). Importantly, canonical NF-κB signaling enhances Wnt signaling, and the interplay of the NF-κB and Wnt pathways induces stem cell–like and tumor-initiating capacities in non–stem cells (Schwitalla et al., 2013). Interestingly, blocking CD70/CD27 signaling reduced the expression of Musashi, an RNA binding protein and Numb repressor. Genetic deletion of Musashi in a mouse model of blast-phase CML signifi-

numbers (A), the frequency and total numbers of human CD45^{dim}SSC^{lo} AML cells (B and C), and total numbers of human CD45^{dim}SSC^{lo}lin$^-$CD90$^-$CD34$^+$ AML stem/progenitor cells (D) in the BM were quantified (FACS). (E) Mean fluorescence intensity (MFI) quotients of CD27 versus isotype on human CD45^{dim}SSC^{lo} lin$^-$CD90$^-$CD34$^+$ AML stem/progenitor cells in the BM (FACS). (F and G) CD11b expression (FACS; F) and Numb intensity (ImageStream^X; G) was determined ex vivo in human CD45^{dim}SSC^{lo} AML blasts (each data point represents pooled cells from $n = 3$ mice). (H and I) 10^3 FACS-sorted human CD45^{dim}SSC^{lo} lin$^-$CD90$^-$CD34$^+$ AML stem/progenitor cells were cultured in methylcellulose. Colony formation (H) and cell numbers per colony (I) were determined after 2 wk. (A–I) Horizontal lines indicate mean. (J and K) 5×10^3 to 10^6 human CD45^{dim}SSC^{lo}lin$^-$CD90$^-$CD34$^+$ AML stem/progenitor cells were FACS-sorted ex vivo from αCD70 or control mAb-treated NSG mice and subjected to mRNA analysis using Fluidigm dynamic array. (J) Heat maps of differentially expressed genes in human AML stem/progenitor cells from individual mice. (K) Gene expression profiles in signaling pathways in human AML stem/progenitor cells regulated by the CD70/CD27 interaction. Log$_2$ fold differences of gene expression levels in signaling pathways (pooled data from all mice in K). Statistics: (A–E, H, and I: unpaired; F and G: paired) Student's t test. *, $P < 0.05$; **, $P < 0.01$; ***, $P < 0.001$; ****, $P < 0.0001$. adv., adverse; fav., favorable; int., intermediate.

cantly reduced leukemia progression (Ito et al., 2010). Earlier results suggested that Musashi might impair asymmetric division and arrest differentiation, partially through suppression of Numb (Imai et al., 2001). The canonical Wnt pathway regulates the expression of Musashi in intestinal epithelial stem cells through a mechanism involving a functional TCF/LEF binding site on its promoter (Rezza et al., 2010). Therefore, it is likely that CD70/CD27 signaling indirectly regulates Musashi via the Wnt pathway.

sCD27 is an important indicator for the CD27/CD70 interaction in vivo. Human sCD27 increased in the AML xenotransplant mice during disease progression, indicating that sCD27 levels represent the strength of CD27 ligation on AML blasts. Importantly, the level of sCD27 in sera of AML patients is an independent negative prognostic factor for overall survival. Serum sCD27 could therefore be used clinically as a surrogate biomarker to address the stemness signature of a patient's AML blasts and to predict outcome. Most likely, CD27 is engaged by CD70 cross-presented by other AML blasts or stem/progenitor cells in a paracrine manner. Alternatively, autocrine CD70/CD27 signaling occurs within the membrane of the same malignant cell. In addition, activated CD70-expressing lymphocytes may trigger CD27 on AML blasts or stem/progenitor cells. Importantly, the CD70/CD27 interaction can be blocked using mAb, leading to prolonged survival in primary and secondary xenotransplantation models. Because αCD70 treatment is specific for malignant cells and does not affect healthy HSPCs, blocking the CD70/CD27 interaction may represent a promising therapeutic strategy for AML.

MATERIALS AND METHODS

Mice

NSG mice were a gift from J. Schwaller (Department of Biomedicine, University Hospital of Basel, Basel, Switzerland) and have been previously described (Shultz et al., 2005). Mice were housed under specific pathogen–free conditions in individually ventilated cages with food and water ad libitum and were regularly monitored for pathogens. Animal experiments were approved by the local experimental animal committee of the Canton of Bern and performed according to Swiss laws for animal protection.

Cell lines

The human leukemia cell lines Kasumi-1 (Asou et al., 1991), HL-60 (Gallagher et al., 1979), PL-21 (Kubonishi et al., 1984), NB4 (Lanotte et al., 1991), HT-93 (Kishi et al., 1998), U-937 (Sundström and Nilsson, 1976), MV4-11 (Lange et al., 1987), MOLM-13 (Matsuo et al., 1997), NOMO-1 (Kato et al., 1986), KG-1 (Koeffler and Golde, 1978), and HEL (Martin and Papayannopoulou, 1982) have been described before.

Patients and controls

Peripheral blood samples ($n = 42$; patient age: 59.9 ± 2.1 yr; morphological blast count: $66.5 \pm 2.8\%$), serum sam-

ples ($n = 137$; patient age: 58.8 ± 1.2 yr; blood leukocyte count: 30.6 ± 4.7 G/liter), and BM aspirates ($n = 25$; patient age: 57.9 ± 3.6 yr; morphological blast infiltration: $72.2 \pm 3.9\%$) were obtained from untreated AML patients at diagnosis at the University Hospital of Bern (Bern, Switzerland) after written informed consent. Study data were collected and managed using REDCap electronic data capture tools hosted at the Department of Clinical Research (Harris et al., 2009). Serum samples were predominantly from a retrospective cohort (2011–2014). Blood, BM, and corresponding serum samples were collected prospectively (2013–2016). Detailed patient and control donor characteristics are listed in Table S1. Peripheral blood samples ($n = 8$; age 29.4 ± 1.8 yr) and serum samples ($n = 5$; age: 30.6 ± 2.1 yr) from young healthy individuals, serum samples ($n = 10$; age: 68.7 ± 2.2 yr) from elderly healthy donors, as well as BM samples from patients who underwent BM biopsy for reasons other than leukemia ($n = 3$; age: 73.3 ± 6.4 yr) were used as controls. Analysis of samples was approved by the local ethical committee of the Canton of Bern.

Antibodies, flow cytometry, and cell purification

αCD27-FITC (clone LG.7F9), αCD27-allophycocyanin (APC)-Cy7 (clone LG.3A10), Armenian hamster IgG-FITC and –APC-Cy7 (clone HTK88), αCD11b-PE-Cy7 (clone M1/70), rat IgG 2bκ-PE-Cy7 (clone RTK4530), αCD34-APC (clone 561), αCD45–Pacific Blue (clone HI30), αCD33-PerCP-Cy5.5 (clone WM53), αCD90-PerCP-Cy5.5 (clone 5E10), and anti–mouse CD45-PE-Cy7 (clone 30-F11) were from BioLegend. Lineage-positive cells were excluded by staining using biotinylated αCD2 (clone RPA2.10), αCD3 (clone OKT39), αCD14 (clone HCD14), αCD16 (clone 3G8), αCD19 (clone HIB19), αCD56 (clone HCD56), and αCD235 (clone HIR2; BioLegend), followed by a second step using streptavidin–Horizon–V500 (BD). αBrdU-APC was from BD. Human αCD70 (clone 41D12-D) and a corresponding control mAb specific for the F protein of respiratory syncytial virus (palivizumab [Synagis]; AstraZeneca) were kindly provided by arGEN-X. CD70 stainings were performed by incubation with 50 µg/ml αCD70 mAb or control mAb followed by a second step using anti–human F_C-PE (BioLegend).

Samples were acquired on an LSRII (BD), and sorting procedures were conducted using an FACSAria (BD). Data were analyzed using FlowJo software (Tree Star).

Antibodies and reagents for treatment

Human αCD27 (clone 1A4) and the corresponding isotype control (clone 15H6) were from Beckman Coulter. Human αCD70 (clone 41D12-D) and palivizumab (Synagis) were from arGEN-X.

Analysis of cell growth

10^5 cells of AML cell lines were seeded into 24-well tissue culture plates and cultured in the presence of 10 µg/ml

blocking αCD27 or αCD70 mAb or the respective control mAb. Live cell numbers were counted daily using a Neubauer chamber and trypan blue exclusion.

Murine xenograft AML model and secondary transplantations

Xenotransplantations were performed as previously described (Sanchez et al., 2009). In brief, NSG mice were sublethally irradiated (2.75 Gy) on the day before injection. 10^6 FACS-purified CD45^{dim}SSC^{lo} blasts from the peripheral blood or BM of newly diagnosed AML patients (patients 142, 145, 161, 162, 163, 164, 167, and 168; Table S1) were injected i.v. into the tail vein. Starting 1–2 wk after transplantation, mice were randomized, and 10 mg/kg αCD70 mAb (41D12-D) or control mAb was administered i.p. every third day. Mice were monitored daily for signs of morbidity (significant weight loss, failure to groom, abnormal gait, and posture) and euthanized when terminally ill. Secondary transplantations were performed by injecting 5×10^6 or 10^7 whole BM cells from primary xenografted animals i.v. into sublethally irradiated (2.75 Gy, day before transplantation) NSG mice.

Liquid cultures and colony assays

In vitro liquid cultures and methylcellulose colony assays of FACS-purified CD45^{dim}SSC^{lo} blasts from blood or BM and CD45^{dim}SSC^{lo}lin$^-$CD90$^-$CD34$^+$ AML stem/progenitor cells from blood of newly diagnosed AML patients (blasts: patients 38, 39, 72, 139, 142, 143, 145, and 146; CD45^{dim} SSC^{lo}lin$^-$CD90$^-$CD34$^+$ AML stem/progenitor cells: patients 161, 162, 163, 164, 167, and 168; Table S1) were performed as described (Schürch et al., 2013), with slight modifications. Starting cell numbers were 10^5 for liquid cultures and 10^3 for colonies, respectively. 10 µg/ml αCD70 or control mAb were added to the cultures in the first round of plating (1°). For each round of serial colony replating (first and second replating), total cells were collected from the methylcellulose, and 5×10^3 cells were replated into methylcellulose without any treatment. Colony numbers were assessed by inverted light microscopy after 2 wk for each round of plating. In one experiment, AML blasts were preincubated overnight with 10^5 irradiated (10 Gy) cells of a CD70-expressing LCL (Ochsenbein et al., 2004), followed by plating in methylcellulose.

Analysis of proliferation in vitro

U-937 cells were cultured in vitro for 72 h, and BrdU (10 µM) was added for the last 4 h of culture. BrdU staining was performed using the APC BrdU Flow kit (BD) according to the manufacturer's instructions.

Lentiviral TCF/LEF reporter assay

U-937 cells were transfected with TCF/LEF lentiviral particles expressing firefly luciferase or the respective positive and negative control lentiviral particles (Cignal Lenti TCF/LEF reporter [luc] kit; SABiosciences) at a multiplicity of infection of 10, in the presence of 8 µg/ml SureEntry transduction

reagent (SABiosciences) according to the manufacturer's instructions. Stable cell lines were generated under puromycin selection (2.5 µg/ml; Santa Cruz Biotechnology, Inc.). Luciferase activity was measured on an Infinite 200 microplate reader (Tecan) using the Steady-Glo Luciferase Assay System (Promega) according to the manufacturer's instructions.

qRT–PCR

For qRT-PCR, total RNA was extracted using the RNeasy Mini kit (QIAGEN). Complementary DNA synthesis was performed using the High Capacity cDNA Reverse Transcription kit (Applied Biosystems). Gene expression analysis was performed using TaqMan Gene Expression Assays for *CD27*, *CD70*, *TNIK*, *CCND1*, *BIRC5*, *TRAF2*, *LEF*, *MYC*, *VEGF*, and *GAPDH* (Applied Biosystems), as well as using self-designed primers for *CEBPA*, *CEBPB*, *RUNX1*, *ID1*, *SPI1* (*PU.1*), and *GAPDH* (Table S2) using SYBR green reaction (Applied Biosystems). qRT-PCR reactions were performed in triplicates including nontemplate controls using an ABI Prism 7500 Sequence Detection System (Applied Biosystems). Relative quantification of gene expression was normalized against a reference gene (*GAPDH*) and calculated as an exponent of 2 ($2^{\Delta Ct}$).

TNIK and β–catenin stainings

AML cells were fixed with 4% paraformaldehyde, followed by blocking and permeabilization with 5% goat serum/1% bovine serum albumin in 0.1% PBS–Tween 20 for 1 h in FACS tubes. After washing, cells were incubated for 1 h with mouse anti–active β-catenin (dilution 1:100; clone 8E7; EMD Millipore) and rabbit αTNIK antibody (dilution 1:50; D-16; Santa Cruz Biotechnology, Inc.), followed by incubation with anti–mouse IgG–Alexa Fluor 546 (dilution 1:500; Invitrogen) and goat anti–rabbit IgG–Alexa-Fluor 488 (dilution: 1:1,000; Cell Signaling Technology) for 30 min. Nuclei were stained with 10 µg/ml DAPI. Cells were acquired on an ImageStream^X Mark II imaging flow cytometer (Amnis/EMD Millipore) and analyzed using INSPIRE and IDEAS software (Amnis/EMD Millipore).

Numb staining and analysis of symmetric versus asymmetric cell division

AML cells were fixed with 4% paraformaldehyde, permeabilized with 1× wash buffer (Dako), and blocked with 10% normal goat serum (Invitrogen) in wash buffer (Dako). Cells were incubated overnight at 4°C with the primary rabbit αNumb antibody (ab14140; Abcam) diluted 1:50 in diluent (Dako). Incubation with the secondary antibody, goat anti–rabbit IgG–Alexa Fluor 568 (dilution 1:1,000; Abcam), was performed for 1 h at room temperature. DAPI (Roche) was used to counterstain for DNA. Samples were acquired on an ImageStream^X Mark II imaging flow cytometer and analyzed using INSPIRE and IDEAS software. Dividing cells were analyzed by IDEAS software in a blinded fashion by two independent researchers. A difference in Numb intensity between

daughter cells of at least 1.8-fold was defined as asymmetric cell division according to Zimdahl et al. (2014).

Knockdown of CD27, TRAF2, and TNIK

CD27, TRAF2, or TNIK was silenced in AML cells using transduction–ready viral particles for gene silencing (Santa Cruz Biotechnology, Inc.). In brief, 5×10^4 cells were transduced overnight at 37°C and 5% CO_2 with 2×10^5 infectious units of shCD27, shTRAF2, or shTNIK lentiviral particles or control scrambled (scr) RNA lentiviral particles (Santa Cruz Biotechnology, Inc.) in the presence of 5 µg/ml polybrene (Sigma-Aldrich) according to the manufacturer's instructions. After 18 h, medium was removed, and cells were cultured in medium supplemented with 2.5 µg/ml puromycin (Santa Cruz Biotechnology, Inc.) to select for stable expression of shRNA or scrRNA. After selection, cells were cultured in medium without antibiotics.

Determination of sCD27 in serum and cell culture supernatants

Human sCD27 in serum samples from newly diagnosed, untreated AML patients, young and elderly healthy controls, and in serum from xenotransplanted NSG mice was measured using the PeliKine Compact human soluble CD27 ELISA kit according to the manufacturer's instructions (Sanquin). For determination of sCD27 in cell culture supernatants, 10^5 FACS-sorted CD45^{dim}SSC^{lo}CD33$^+$ AML blasts or CD45^{dim}SSC^{lo}lin$^-$CD90$^-$CD34$^+$ AML stem/progenitor cells were cultured in liquid culture in 96-well V-bottom plates in the presence of 10 µg/ml αCD70 or control mAb for 3 d. sCD27 in supernatants was measured using the PeliKine Compact human soluble CD27 ELISA kit.

Gene expression profiling using Fluidigm dynamic array

10^5 FACS-sorted CD45^{dim}SSC^{lo}CD33$^+$ blasts from the blood or BM of 20 different newly diagnosed AML patients were cultured in vitro in the presence of αCD70 or control mAb for 72 h, or CD45$^+$lin$^-$CD90$^-$CD34$^+$ AML stem/progenitor cells were FACS-sorted ex vivo from αCD70- or control mAb–treated NSG mice. Cells were subjected to simultaneous isolation of DNA, RNA, and proteins using the AllPrep DNA/RNA/Protein Mini kit (QIAGEN) according to an optimized protocol (Radpour et al., 2009, 2011). The quantity of extracted molecules was assessed by spectrophotometry using a NanoDrop ND-1000 (Thermo Fisher Scientific). For RNA samples, complementary DNA synthesis was performed using the High Capacity cDNA Reverse Transcription kit (Applied Biosystems). Gene expression profiling was performed on sample duplicates using the 96.96 Biomark Dynamic Array (Fluidigm) according to the manufacturer's advanced protocol (Wong et al., 2010). Assays were designed based on EvaGreen chemistry (Biotium), and primers for targeting desired pathways were designed accordingly for amplicons of 100–150 bp using Primer3Plus (Table S2; Untergasser et al., 2007). In brief,

cDNA was subjected to preamplification (specific target amplification [STA]) with a mix of primers specific for the target genes. STA was performed by denaturing at 95°C for 15 s and annealing/amplification at 60°C for 4 min, which was repeated for 15 cycles. STA products were then diluted fivefold in DNA suspension buffer according to the manufacturer's instructions (Fluidigm) and supplemented with TaqMan Gene Expression Master Mix (Thermo Fisher Scientific) and EvaGreen DNA binding dye (Biotium). Samples and primers were loaded into the integrated fluidic circuits of the 96.96 Dynamic Array, and analysis was performed on a BioMark HD System (Fluidigm). Cycle threshold (Ct) values were calculated and visualized using BioMark real-time PCR analysis software (Fluidigm).

As a quality-control measure, we removed genes with Ct values of ≥32.0 or differences of ≥2.0 in-between sample duplicates. If the reference genes (*ACTB* and *GAPDH*) were not expressed or were removed because of the aforementioned criteria, the sample was not included in further analysis.

Raw values were normalized using the geometric mean of the two reference genes (*ACTB* and *GAPDH*). The fold difference for each sample was calculated using the comparative Ct method (Livak and Schmittgen, 2001). Relative gene expression quantities after log$_2$ transformation were used for unsupervised hierarchical clustering of differentially expressed genes using standard Pearson's correlation as similarity measurement and Ward's method for clustering the data (Radpour et al., 2011).

GO enrichment analysis

GO enrichment was assessed using Genomics Suite software, version 6.6 (Partek Inc.). The list of significantly differently expressed genes was grouped into functional hierarchies, and enrichment scores were calculated using a χ^2 test comparing the proportion of the gene list in a group to the proportion of the background in the group. A value of three or higher corresponds to differential expression of a pathway ($P < 0.05$).

Cell signaling and in silico pathway analysis

Gene networks and canonical pathways representing differentially expressed genes were identified using the Ariadne Genomics Pathway Studio software, version 9 (Elsevier). The dataset containing gene identifiers and corresponding fold changes was uploaded into the Pathway Studio. The functional analysis identified the direct interactions between differentially expressed genes and selected pathways to facilitate the understanding beyond their regulatory networks.

Microarray data

Expression data were derived from a public repository for microarray data (GEO) and are available under accession nos. GSE4170 (Radich et al., 2006), GSE12417 (Metzeler et al., 2008), and GSE1159 (Valk et al., 2004).

Statistical analysis

Statistical analysis was performed using Prism 5.0 (Graph-Pad Software) and SAS 9.3 (SAS Institute). Data are represented as mean ± SEM. Data were analyzed using one-way ANOVA and Tukey's or Dunnett's multiple comparison test, two-way ANOVA, and Bonferroni post-test, unpaired or paired Student's t test (two-tailed), or Mann–Whitney test. Receiver operating characteristic curve analysis was used to identify the optimal threshold for sCD27 for subsequent survival analysis. In brief, 30% of the entire patient cohort ($n = 41$) was randomly selected, and receiver operating characteristic curve analysis was performed. To verify the reliability of the cutoff, 200 bootstrapped replications were performed. Next, all patients were then classified as low or high according to the cutoff. Univariate survival analysis was performed. Survival time differences were plotted using Kaplan–Meier curves and analyzed using the log–rank test. After verification of the proportional hazards assumption, multiple Cox regression analysis was performed using the continuous sCD27 values. Effect size was determined using hazard ratios (HRs) and 95% confidence intervals, with a baseline hazard of 1.0 and a greater risk of death with HR >1.0. All P values were two-sided and considered significant when $P < 0.05$.

Online supplemental material

Fig. S1 shows the FACS gating strategy to identify the CD45^{dim}SSC^{lo} blast gate in healthy individuals and the gating strategy for AML CD45^{dim}SSC^{lo}lin^{−}CD90^{−}CD34^{+} stem/progenitor cells. Table S1 lists the characteristics of AML patients, healthy controls, and patients who underwent BM biopsy for other reasons than leukemia. Table S2 lists the primer sequences used for qRT-PCR and the 96.96 Biomark Dynamic Array.

REFERENCES

Aoun, P., and S.J. Pirruccello. 2007. Hematopoietic cell differentiation: Monoclonal antibodies and cluster designation defined hematopoietic cell antigens. *In* Flow Cytometry in Clinical Diagnosis. Fourth edition. J.L. Carey, J.P. McCoy, and D.F. Keren, editors. American Society for Clinical Pathology, Chicago. 35–54.

Asou, H., S. Tashiro, K. Hamamoto, A. Otsuji, K. Kita, and N. Kamada. 1991. Establishment of a human acute myeloid leukemia cell line (Kasumi-1) with 8;21 chromosome translocation. *Blood.* 77:2031–2036.

Bajaj, J., B. Zimdahl, and T. Reya. 2015. Fearful symmetry: subversion of asymmetric division in cancer development and progression. *Cancer Res.* 75:792–797. http://dx.doi.org/10.1158/0008-5472.CAN-14-2750

Bartholdy, B., M. Christopeit, B. Will, Y. Mo, L. Barreyro, Y. Yu, T.D. Bhagat, U.C. Okoye-Okafor, T.I. Todorova, J.M. Greally, et al. 2014. HSC commitment-associated epigenetic signature is prognostic in acute myeloid leukemia. *J. Clin. Invest.* 124:1158–1167. http://dx.doi.org/10.1172/JCI71264

Ben-Porath, I., M.W. Thomson, V.J. Carey, R. Ge, G.W. Bell, A. Regev, and R.A. Weinberg. 2008. An embryonic stem cell-like gene expression signature in poorly differentiated aggressive human tumors. *Nat. Genet.* 40:499–507. http://dx.doi.org/10.1038/ng.127

Blair, A., D.E. Hogge, L.E. Ailles, P.M. Lansdorp, and H.J. Sutherland. 1997. Lack of expression of Thy-1 (CD90) on acute myeloid leukemia cells with long-term proliferative ability in vitro and in vivo. *Blood.* 89:3104–3112.

Bonnet, D., and J.E. Dick. 1997. Human acute myeloid leukemia is organized as a hierarchy that originates from a primitive hematopoietic cell. *Nat. Med.* 3:730–737. http://dx.doi.org/10.1038/nm0797-730

Borowitz, M.J., K.L. Guenther, K.E. Shults, and G.T. Stelzer. 1993. Immunophenotyping of acute leukemia by flow cytometric analysis. Use of CD45 and right-angle light scatter to gate on leukemic blasts in three-color analysis. *Am. J. Clin. Pathol.* 100:534–540. http://dx.doi.org/10.1093/ajcp/100.5.534

Clevers, H., and R. Nusse. 2012. Wnt/β-catenin signaling and disease. *Cell.* 149:1192–1205. http://dx.doi.org/10.1016/j.cell.2012.05.012

Corces-Zimmerman, M.R., W.J. Hong, I.L. Weissman, B.C. Medeiros, and R. Majeti. 2014. Preleukemic mutations in human acute myeloid leukemia affect epigenetic regulators and persist in remission. *Proc. Natl. Acad. Sci. USA.* 111:2548–2553. http://dx.doi.org/10.1073/pnas.1324297111

Döhner, H., D.J. Weisdorf, and C.D. Bloomfield. 2015. Acute myeloid leukemia. *N. Engl. J. Med.* 373:1136–1152. http://dx.doi.org/10.1056/NEJMra1406184

Eppert, K., K. Takenaka, E.R. Lechman, L. Waldron, B. Nilsson, P. van Galen, K.H. Metzeler, A. Poeppl, V. Ling, J. Beyene, et al. 2011. Stem cell gene expression programs influence clinical outcome in human leukemia. *Nat. Med.* 17:1086–1093. http://dx.doi.org/10.1038/nm.2415

Figueroa, M.E., S. Lugthart, Y. Li, C. Erpelinck-Verschueren, X. Deng, P.J. Christos, E. Schifano, J. Booth, W. van Putten, L. Skrabanek, et al. 2010. DNA methylation signatures identify biologically distinct subtypes in acute myeloid leukemia. *Cancer Cell.* 17:13–27. http://dx.doi.org/10.1016/j.ccr.2009.11.020

Gallagher, R., S. Collins, J. Trujillo, K. McCredie, M. Ahearn, S. Tsai, R. Metzgar, G. Aulakh, R. Ting, F. Ruscetti, and R. Gallo. 1979. Characterization of

the continuous, differentiating myeloid cell line (HL-60) from a patient with acute promyelocytic leukemia. *Blood*. 54:713–733.

Gentles, A.J., S.K. Plevritis, R. Majeti, and A.A. Alizadeh. 2010. Association of a leukemic stem cell gene expression signature with clinical outcomes in acute myeloid leukemia. *JAMA*. 304:2706–2715. http://dx.doi.org/10.1001/jama.2010.1862

George, T.C., S.L. Fanning, P. Fitzgerald-Bocarsly, R.B. Medeiros, S. Highfill, Y. Shimizu, B.E. Hall, K. Frost, D. Basiji, W.E. Ortyn, et al. 2006. Quantitative measurement of nuclear translocation events using similarity analysis of multispectral cellular images obtained in flow. *J. Immunol. Methods*. 311:117–129. (published erratum appears in *J. Immunol. Methods*. 2009. 344:85) http://dx.doi.org/10.1016/j.jim.2006.01.018

Gorczyca, W. 2010. Flow Cytometry in Neoplastic Hematology: Morphologic–Immunophenotypic Correlation. Second edition. Informa UK, London. 358 pp. http://dx.doi.org/10.3109/9781841847443

Grewal, I.S. 2008. CD70 as a therapeutic target in human malignancies. *Expert Opin. Ther. Targets*. 12:341–351. http://dx.doi.org/10.1517/14728222.12.3.341

Grimwade, D., A.R. Mistry, E. Solomon, and F. Guidez. 2010. Acute promyelocytic leukemia: a paradigm for differentiation therapy. *Cancer Treat. Res*. 145:219–235. http://dx.doi.org/10.1007/978-0-387-69259-3_13

Harris, P.A., R. Taylor, R. Thielke, J. Payne, N. Gonzalez, and J.G. Conde. 2009. Research electronic data capture (REDCap)—a metadata-driven methodology and workflow process for providing translational research informatics support. *J. Biomed. Inform*. 42:377–381. http://dx.doi.org/10.1016/j.jbi.2008.08.010

Heidel, F.H., L. Bullinger, Z. Feng, Z. Wang, T.A. Neff, L. Stein, D. Kalaitzidis, S.W. Lane, and S.A. Armstrong. 2012. Genetic and pharmacologic inhibition of β-catenin targets imatinib-resistant leukemia stem cells in CML. *Cell Stem Cell*. 10:412–424. http://dx.doi.org/10.1016/j.stem.2012.02.017

Horton, S.J., and B.J. Huntly. 2012. Recent advances in acute myeloid leukemia stem cell biology. *Haematologica*. 97:966–974. http://dx.doi.org/10.3324/haematol.2011.054734

Huntly, B.J., and D.G. Gilliland. 2005. Leukaemia stem cells and the evolution of cancer-stem-cell research. *Nat. Rev. Cancer*. 5:311–321. http://dx.doi.org/10.1038/nrc1592

Imai, T., A. Tokunaga, T. Yoshida, M. Hashimoto, K. Mikoshiba, G. Weinmaster, M. Nakafuku, and H. Okano. 2001. The neural RNA-binding protein Musashi1 translationally regulates mammalian numb gene expression by interacting with its mRNA. *Mol. Cell. Biol*. 21:3888–3900. http://dx.doi.org/10.1128/MCB.21.12.3888-3900.2001

Ito, T., H.Y. Kwon, B. Zimdahl, K.L. Congdon, J. Blum, W.E. Lento, C. Zhao, A. Lagoo, G. Gerrard, L. Foroni, et al. 2010. Regulation of myeloid leukaemia by the cell-fate determinant Musashi. *Nature*. 466:765–768. http://dx.doi.org/10.1038/nature09171

Jamieson, C.H., L.E. Ailles, S.J. Dylla, M. Muijtjens, C. Jones, J.L. Zehnder, J. Gotlib, K. Li, M.G. Manz, A. Keating, et al. 2004. Granulocyte-macrophage progenitors as candidate leukemic stem cells in blast-crisis CML. *N. Engl. J. Med*. 351:657–667. http://dx.doi.org/10.1056/NEJMoa040258

Jan, M., T.M. Snyder, M.R. Corces-Zimmerman, P. Vyas, I.L. Weissman, S.R. Quake, and R. Majeti. 2012. Clonal evolution of preleukemic hematopoietic stem cells precedes human acute myeloid leukemia. *Sci. Transl. Med*. 4:149ra118. http://dx.doi.org/10.1126/scitranslmed.3004315

Kato, Y., M. Ogura, M. Okumura, Y. Morishima, T. Horita, and R. Ohno. 1986. Establishment of peroxidase positive, human monocytic leukemia cell line (NOMO-1) and its characteristics. *Acta Haematol Jpn*. 49:277.

Kishi, K., K. Toba, T. Azegami, N. Tsukada, Y. Uesugi, M. Masuko, H. Niwano, S. Hashimoto, M. Sakaue, T. Furukawa, et al. 1998. Hematopoietic cyto-kine-dependent differentiation to eosinophils and neutrophils in a newly established acute promyelocytic leukemia cell line with t(15;17). *Exp. Hematol*. 26:135–142.

Koeffler, H.P., and D.W. Golde. 1978. Acute myelogenous leukemia: a human cell line responsive to colony-stimulating activity. *Science*. 200:1153–1154. http://dx.doi.org/10.1126/science.306682

Kreso, A., and J.E. Dick. 2014. Evolution of the cancer stem cell model. *Cell Stem Cell*. 14:275–291. http://dx.doi.org/10.1016/j.stem.2014.02.006

Krivtsov, A.V., and S.A. Armstrong. 2007. MLL translocations, histone modifications and leukaemia stem-cell development. *Nat. Rev. Cancer*. 7:823–833. http://dx.doi.org/10.1038/nrc2253

Kroft, S.H., and N.J. Karandikar. 2007. Flow cytometric analysis of acute leukemias, myelodysplastic syndromes, and myeloproliferative disorders. *In* Flow Cytometry in Clinical Diagnosis. Fourth edition. J.L. Carey, J.P. McCoy, and D.F. Keren, editors. American Society for Clinical Pathology, Chicago. 168–214.

Kubonishi, I., K. Machida, K. Niiya, H. Sonobe, Y. Ohtsuki, K. Iwata, and I. Miyoshi. 1984. Establishment of a new peroxidase-positive human my-eloid cell line, PL-21. *Blood*. 63:254–259.

Lange, B., M. Valtieri, D. Santoli, D. Caracciolo, F. Mavilio, I. Gemperlein, C. Griffin, B. Emanuel, J. Finan, P. Nowell, et al. 1987. Growth factor requirements of childhood acute leukemia: establishment of GM-CSF-dependent cell lines. *Blood*. 70:192–199.

Lanotte, M., V. Martin-Thouvenin, S. Najman, P. Balerini, F. Valensi, and R. Berger. 1991. NB4, a maturation inducible cell line with t(15;17) marker isolated from a human acute promyelocytic leukemia (M3). *Blood*. 77:1080–1086.

Livak, K.J., and T.D. Schmittgen. 2001. Analysis of relative gene expression data using real-time quantitative PCR and the $2^{-\Delta\Delta C(T)}$ method. *Methods*. 25:402–408. http://dx.doi.org/10.1006/meth.2001.1262

Mahmoudi, T., V.S. Li, S.S. Ng, N. Taouatas, R.G. Vries, S. Mohammed, A.J. Heck, and H. Clevers. 2009. The kinase TNIK is an essential activator of Wnt target genes. *EMBO J*. 28:3329–3340. http://dx.doi.org/10.1038/emboj.2009.285

Majeti, R., C.Y. Park, and I.L. Weissman. 2007. Identification of a hierarchy of multipotent hematopoietic progenitors in human cord blood. *Cell Stem Cell*. 1:635–645. http://dx.doi.org/10.1016/j.stem.2007.10.001

Martin, P., and T. Papayannopoulou. 1982. HEL cells: a new human erythroleukemia cell line with spontaneous and induced globin expression. *Science*. 216:1233–1235. http://dx.doi.org/10.1126/science.6177045

Matsuo, Y., R.A. MacLeod, C.C. Uphoff, H.G. Drexler, C. Nishizaki, Y. Katayama, G. Kimura, N. Fujii, E. Omoto, M. Harada, and K. Orita. 1997. Two acute monocytic leukemia (AML-M5a) cell lines (MOLM-13 and MOLM-14) with interclonal phenotypic heterogeneity showing MLL-AF9 fusion resulting from an occult chromosome insertion, ins(11;9)(q23;p22p23). *Leukemia*. 11:1469–1477. http://dx.doi.org/10.1038/sj.leu.2400768

Metzeler, K.H., M. Hummel, C.D. Bloomfield, K. Spiekermann, J. Braess, M.C. Sauerland, A. Heinecke, M. Radmacher, G. Marcucci, S.P. Whitman, et al. German AML Cooperative Group. 2008. An 86-probe-set gene-expression signature predicts survival in cytogenetically normal acute myeloid leukemia. *Blood*. 112:4193–4201. http://dx.doi.org/10.1182/blood-2008-02-134411

Metzeler, K.H., K. Maharry, J. Kohlschmidt, S. Volinia, K. Mrózek, H. Becker, D. Nicolet, S.P. Whitman, J.H. Mendler, S. Schwind, et al. 2013. A stem cell-like gene expression signature associates with inferior outcomes and a distinct microRNA expression profile in adults with primary cytogenetically normal acute myeloid leukemia. *Leukemia*. 27:2023–2031. http://dx.doi.org/10.1038/leu.2013.181

Nolte, M.A., R. Arens, R. van Os, M. van Oosterwijk, B. Hooibrink, R.A. van Lier, and M.H. van Oers. 2005. Immune activation modulates hematopoiesis through interactions between CD27 and CD70. *Nat. Immunol.* 6:412–418. http://dx.doi.org/10.1038/ni1174

Nolte, M.A., R.W. van Olffen, K.P. van Gisbergen, and R.A. van Lier. 2009. Timing and tuning of CD27-CD70 interactions: the impact of signal strength in setting the balance between adaptive responses and immunopathology. *Immunol. Rev.* 229:216–231. http://dx.doi.org/10.1111/j.1600-065X.2009.00774.x

Nowak, D., D. Stewart, and H.P. Koeffler. 2009. Differentiation therapy of leukemia: 3 decades of development. *Blood.* 113:3655–3665. http://dx.doi.org/10.1182/blood-2009-01-198911

Ochsenbein, A.F., S.R. Riddell, M. Brown, L. Corey, G.M. Baerlocher, P.M. Lansdorp, and P.D. Greenberg. 2004. CD27 expression promotes long-term survival of functional effector-memory CD8^{+} cytotoxic T lymphocytes in HIV-infected patients. *J. Exp. Med.* 200:1407–1417. http://dx.doi.org/10.1084/jem.20040717

Patel, J.P., M. Gönen, M.E. Figueroa, H. Fernandez, Z. Sun, J. Racevskis, P. Van Vlierberghe, I. Dolgalev, S. Thomas, O. Aminova, et al. 2012. Prognostic relevance of integrated genetic profiling in acute myeloid leukemia. *N. Engl. J. Med.* 366:1079–1089. http://dx.doi.org/10.1056/NEJMoa1112304

Pearce, D.J., D. Taussig, K. Zibara, L.L. Smith, C.M. Ridler, C. Preudhomme, B.D. Young, A.Z. Rohatiner, T.A. Lister, and D. Bonnet. 2006. AML engraftment in the NOD/SCID assay reflects the outcome of AML: implications for our understanding of the heterogeneity of AML. *Blood.* 107:1166–1173. http://dx.doi.org/10.1182/blood-2005-06-2325

Radich, J.P., H. Dai, M. Mao, V. Oehler, J. Schelter, B. Druker, C. Sawyers, N. Shah, W. Stock, C.L. Willman, et al. 2006. Gene expression changes associated with progression and response in chronic myeloid leukemia. *Proc. Natl. Acad. Sci. USA.* 103:2794–2799. http://dx.doi.org/10.1073/pnas.0510423103

Radpour, R., M. Sikora, T. Grussenmeyer, C. Kohler, Z. Barekati, W. Holzgreve, I. Lefkovits, and X.Y. Zhong. 2009. Simultaneous isolation of DNA, RNA, and proteins for genetic, epigenetic, transcriptomic, and proteomic analysis. *J. Proteome Res.* 8:5264–5274. http://dx.doi.org/10.1021/pr900591w

Radpour, R., Z. Barekati, C. Kohler, M.M. Schumacher, T. Grussenmeyer, P. Jenoe, N. Hartmann, S. Moes, M. Letzkus, J. Bitzer, et al. 2011. Integrated epigenetics of human breast cancer: synoptic investigation of targeted genes, microRNAs and proteins upon demethylation treatment. *PLoS One.* 6:e27355. http://dx.doi.org/10.1371/journal.pone.0027355

Reya, T., S.J. Morrison, M.F. Clarke, and I.L. Weissman. 2001. Stem cells, cancer, and cancer stem cells. *Nature.* 414:105–111. http://dx.doi.org/10.1038/35102167

Rezza, A., S. Skah, C. Roche, J. Nadjar, J. Samarut, and M. Plateroti. 2010. The overexpression of the putative gut stem cell marker Musashi-1 induces tumorigenesis through Wnt and Notch activation. *J. Cell Sci.* 123:3256–3265. http://dx.doi.org/10.1242/jcs.065284

Riether, C., C.M. Schürch, C. Flury, M. Hinterbrandner, L. Drück, A.L. Huguenin, G.M. Baerlocher, R. Radpour, and A.F. Ochsenbein. 2015. Tyrosine kinase inhibitor–induced CD70 expression mediates drug resistance in leukemia stem cells by activating Wnt signaling. *Sci. Transl. Med.* 7:298ra119. http://dx.doi.org/10.1126/scitranslmed.aab1740

Rosenbauer, F., and D.G. Tenen. 2007. Transcription factors in myeloid development: balancing differentiation with transformation. *Nat. Rev. Immunol.* 7:105–117. http://dx.doi.org/10.1038/nri2024

Sanchez, P.V., R.L. Perry, J.E. Sarry, A.E. Perl, K. Murphy, C.R. Swider, A. Bagg, J.K. Choi, J.A. Biegel, G. Danet-Desnoyers, and M. Carroll. 2009. A robust xenotransplantation model for acute myeloid leukemia. *Leukemia.* 23:2109–2117. http://dx.doi.org/10.1038/leu.2009.143

Sarry, J.E., K. Murphy, R. Perry, P.V. Sanchez, A. Secreto, C. Keefer, C.R. Swider, A.C. Strzelecki, C. Cavelier, C. Récher, et al. 2011. Human acute myelogenous leukemia stem cells are rare and heterogeneous when assayed in NOD/SCID/IL2Rγc-deficient mice. *J. Clin. Invest.* 121:384–395. http://dx.doi.org/10.1172/JCI41495

Schürch, C., C. Riether, M.S. Matter, A. Tzankov, and A.F. Ochsenbein. 2012. CD27 signaling on chronic myelogenous leukemia stem cells activates Wnt target genes and promotes disease progression. *J. Clin. Invest.* 122:624–638. http://dx.doi.org/10.1172/JCI45977

Schürch, C., C. Riether, M.A. Amrein, and A.F. Ochsenbein. 2013. Cytotoxic T cells induce proliferation of chronic myeloid leukemia stem cells by secreting interferon-γ. *J. Exp. Med.* 210:605–621. http://dx.doi.org/10.1084/jem.20121229

Schwitalla, S., A.A. Fingerle, P. Cammareri, T. Nebelsiek, S.I. Göktuna, P.K. Ziegler, O. Canli, J. Heijmans, D.J. Huels, G. Moreaux, et al. 2013. Intestinal tumorigenesis initiated by dedifferentiation and acquisition of stem-cell-like properties. *Cell.* 152:25–38. http://dx.doi.org/10.1016/j.cell.2012.12.012

Shlush, L.I., S. Zandi, A. Mitchell, W.C. Chen, J.M. Brandwein, V. Gupta, J.A. Kennedy, A.D. Schimmer, A.C. Schuh, K.W. Yee, et al. HALT Pan-Leukemia Gene Panel Consortium. 2014. Identification of pre-leukaemic haematopoietic stem cells in acute leukaemia. *Nature.* 506:328–333. (published erratum appears in *Nature.* 2014. 508:420) http://dx.doi.org/10.1038/nature13038

Shultz, L.D., B.L. Lyons, L.M. Burzenski, B. Gott, X. Chen, S. Chaleff, M. Kotb, S.D. Gillies, M. King, J. Mangada, et al. 2005. Human lymphoid and myeloid cell development in NOD/LtSz-scid IL2R gamma null mice engrafted with mobilized human hemopoietic stem cells. *J. Immunol.* 174:6477–6489. http://dx.doi.org/10.4049/jimmunol.174.10.6477

Siegel, R., D. Naishadham, and A. Jemal. 2013. Cancer statistics, 2013. *CA Cancer J. Clin.* 63:11–30. http://dx.doi.org/10.3322/caac.21166

Silence, K., T. Dreier, M. Moshir, P. Ulrichts, S.M. Gabriels, M. Saunders, H. Wajant, P. Brouckaert, L. Huyghe, T. Van Hauwermeiren, et al. 2014. ARGX-110, a highly potent antibody targeting CD70, eliminates tumors via both enhanced ADCC and immune checkpoint blockade. *MAbs.* 6:523–532. http://dx.doi.org/10.4161/mabs.27398

Staal, F.J., and H.C. Clevers. 2005. WNT signalling and haematopoiesis: a WNT-WNT situation. *Nat. Rev. Immunol.* 5:21–30. http://dx.doi.org/10.1038/nri1529

Sundström, C., and K. Nilsson. 1976. Establishment and characterization of a human histiocytic lymphoma cell line (U-937). *Int. J. Cancer.* 17:565–577. http://dx.doi.org/10.1002/ijc.2910170504

Tenen, D.G. 2003. Disruption of differentiation in human cancer: AML shows the way. *Nat. Rev. Cancer.* 3:89–101. http://dx.doi.org/10.1038/nrc989

Terwijn, M., W. Zeijlemaker, A. Kelder, A.P. Rutten, A.N. Snel, W.J. Scholten, T. Pabst, G. Verhoef, B. Löwenberg, S. Zweegman, et al. 2014. Leukemic stem cell frequency: a strong biomarker for clinical outcome in acute myeloid leukemia. *PLoS One.* 9:e107587. http://dx.doi.org/10.1371/journal.pone.0107587

Untergasser, A., H. Nijveen, X. Rao, T. Bisseling, R. Geurts, and J.A. Leunissen. 2007. Primer3Plus, an enhanced web interface to Primer3. *Nucleic Acids Res.* 35:W71–W74. http://dx.doi.org/10.1093/nar/gkm306

Valk, P.J., R.G. Verhaak, M.A. Beijen, C.A. Erpelinck, S. Barjesteh van Waalwijk van Doorn-Khosrovani, J.M. Boer, H.B. Beverloo, M.J. Moorhouse, P.J. van der Spek, B. Löwenberg, and R. Delwel. 2004. Prognostically useful gene-expression profiles in acute myeloid leukemia. *N. Engl. J. Med.* 350:1617–1628. http://dx.doi.org/10.1056/NEJMoa040465

van Rhenen, A., N. Feller, A. Kelder, A.H. Westra, E. Rombouts, S. Zweegman, M.A. van der Pol, Q. Waisfisz, G.J. Ossenkoppele, and G.J. Schuurhuis. 2005. High stem cell frequency in acute myeloid leukemia at diagnosis predicts high minimal residual disease and poor survival. *Clin. Cancer Res.* 11:6520–6527. http://dx.doi.org/10.1158/1078-0432.CCR-05-0468

Vasanthakumar, A., and L.A. Godley. 2014. On the origin of leukemic species. *Cell Stem Cell*. 14:421–422. http://dx.doi.org/10.1016/j.stem.2014.03.008

Wang, Y., A.V. Krivtsov, A.U. Sinha, T.E. North, W. Goessling, Z. Feng, L.I. Zon, and S.A. Armstrong. 2010. The Wnt/β-catenin pathway is required for the development of leukemia stem cells in AML. *Science*. 327:1650–1653. http://dx.doi.org/10.1126/science.1186624

Wong, C.C., K.E. Loewke, N.L. Bossert, B. Behr, C.J. De Jonge, T.M. Baer, and R.A. Reijo Pera. 2010. Non-invasive imaging of human embryos before embryonic genome activation predicts development to the blastocyst stage. *Nat. Biotechnol.* 28:1115–1121. http://dx.doi.org/10.1038/nbt.1686

Wu, M., H.Y. Kwon, F. Rattis, J. Blum, C. Zhao, R. Ashkenazi, T.L. Jackson, N. Gaiano, T. Oliver, and T. Reya. 2007. Imaging hematopoietic precursor division in real time. *Cell Stem Cell*. 1:541–554. http://dx.doi.org/10.1016/j.stem.2007.08.009

Zeisig, B.B., A.G. Kulasekararaj, G.J. Mufti, and C.W. So. 2012. SnapShot: Acute myeloid leukemia. *Cancer Cell*. 22:698–698.e1. http://dx.doi.org/10.1016/j.ccr.2012.10.017

Zimdahl, B., T. Ito, A. Blevins, J. Bajaj, T. Konuma, J. Weeks, C.S. Koechlein, H.Y. Kwon, O. Arami, D. Rizzieri, et al. 2014. Lis1 regulates asymmetric division in hematopoietic stem cells and in leukemia. *Nat. Genet.* 46:245–252. http://dx.doi.org/10.1038/ng.2889